

# ELECTRON DISTRIBUTION IN THE IONOSPHERE\*

N66 37957

ROBERT E. BOURDEAU

## 1. INTRODUCTION

Under average conditions, the electrons with thermal energies that form the ionosphere result from photoionization of the upper atmosphere by ultraviolet and x-radiation from the sun and possibly by corpuscular radiation. These electrons are lost by recombination with ions simultaneously produced. The loss rate is slow enough that the ionosphere persists throughout the night especially at the higher altitudes.

In addition to the above-described production and loss mechanisms, gravitational and electromagnetic forces contribute to the determination of the altitude distribution of electrons the combination of all these factors is such that several regions with distinctive features are formed. This natural subdivision permits a discussion of the ionospheric electron distribution to be subdivided accordingly. Specifically, as will be done here, it allows for separate discussions of the D (50–85 kilometers), the E (85–140 km) and the F (140–1000 km) regions and of the outer ionosphere which extends from 1000 km to several earth radii.

The electron density ( $N_e$ ) typically varies from  $10^3\text{cm}^{-3}$  in the D region, to  $10^5\text{cm}^{-3}$  in the E region, reaches a maximum of  $10^6\text{cm}^{-3}$  at 300 km in the F region and then decreases monotonically to  $10\text{cm}^{-3}$  at a distance of several earth radii. The principal changes from a given electron density profile will occur with time of day, with season, with temporal position within the solar cycle and with latitude. The relative importance of each of these effects depends upon the ionospheric subdivision under discussion. The dynamic nature of the ionosphere is evidenced by the fact that one of these effects can produce an order of

magnitude variation in  $N_e$  at specified altitudes. The problem of orderly discussion is complicated further by the very large variations that result from solar storms and from energetic particle precipitation into the auroral region.

In organizing the discussion, it would have been natural to choose a condition of maximum or minimum solar activity and then treat the variations about it. However, observational evidence at least for the regions below 85 and above 300 km is weighted heavily toward the middle of the current solar cycle. For this reason, the term "average profile" is used here for a noontime, mid-latitude ionosphere at an epoch midway between solar maximum and solar minimum conditions. "Average profiles" will be developed for each of the four subdivisions prior to discussions of temporal and latitudinal changes about them. Solar storm and auroral phenomena shall be discussed but treated as special events.

## 2. AN AVERAGE D REGION ELECTRON DENSITY PROFILE

The D region, even though the most accessible, is the most difficult to study experimentally because it contains the lowest ratio of electron to neutral gas density. The difficulty principally is embodied in the separation of the electron density and collision frequency parameters, which simultaneously contribute to measured phenomena. Separation of these two parameters has been accomplished by experiments involving radio propagation between the earth and a rocket. Ground-based experiments have been carried out by cross-modulation and partial-reflection techniques. One common denominator of ground-based methods is that the altitude dependence of electron density is extracted from the experimental data only by assuming an electron collision

\*Published as *Goddard Space Flight Center Document X-615-64-29*, January 1964. This work was also published in "International Dictionary of Geophysics" Pergamon Press, Oxford, England

frequency profile, usually that measured with rocket experiments by Kane (1961). Rocket-borne dc probes have been used but the theoretical analysis is based on the assumption of a collision-free plasma sheath, an unlikely condition at D region altitudes.

Few D region profiles have been reported for the "average" conditions. An average profile applicable to a quiet midday ionosphere is pre-

would be considered mid-latitudes from the standpoint of a neutral atmosphere. However, it must be emphasized that most of the results were obtained at magnetic dips greater than  $70^\circ$ . Consequently, it justifiably could be argued from the viewpoint of ionospheric physics that the profile is more representative of polar conditions, in the absence of solar storms and of auroral and magnetic disturbances.

### 3. VARIATIONS FROM THE AVERAGE D REGION ELECTRON DENSITY PROFILE

Observational D region data are so sparse that temporal and latitudinal variations are principally hypothetical. Excluding special events, the *diurnal* variation is the major effect, the D region being essentially non-existent at night, at least from the standpoint of the  $N_e$  parameter. The results of Barrington et al (1962) indicate rapid formation of the D region just after layer sunrise.

We only can conjecture about the *solar cycle* variation at this time. If the prevailing theory\* for D region formation is correct, then a solar cycle change of less than a factor of two in the entire reference  $N_e$  profile would be expected because of the relative constancy of the responsible ionizing radiation (cosmic rays below 70 km and Lyman alpha radiation between 70 and 85 km). Moderate (less than a factor of 2) *latitude* variations should exist in the lower D region, in accordance with the latitudinal dependence of the flux of cosmic rays.

We turn now to the large electron density enhancements that occur in the D region during special events and which generally are associated with radio-blackouts. Belrose and Cetiner (1962) have measured the enhancement during a Sudden Ionosphere Disturbance\* (Curve B of Figure 1), an event occurring on the sunlit side of the earth simultaneously with the appearance of a flare and having a time duration of about one hour. It is seen that there is a general increase in  $N_e$  of about a factor of 10 during such periods of enhanced X-ray activity. Even larger electron density increases have been observed with rocket experiments flown in connection with high latitude phenomena. Jespersen et al (1963) have obtained  $N_e$  data during an auroral absorption

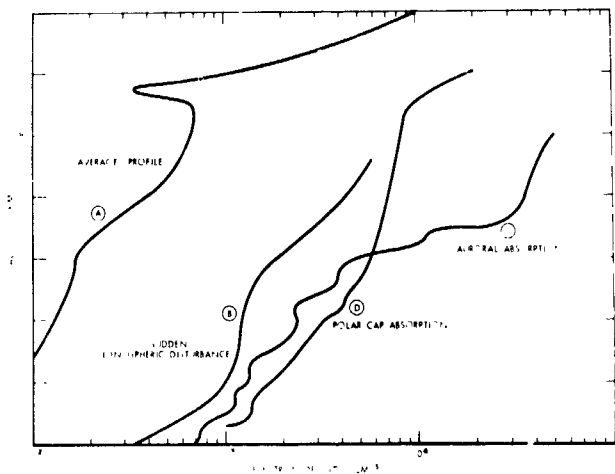


FIGURE 1.—D region electron density profiles

sented as curve A in Figure 1. It was constructed from the space flight results of Aikin et al (1963) and of Hall (1963) and from the ground-based observations of Belrose (1961) and of Barrington et al (1962). Except for the latter results above 75 km, there is agreement to better than a factor of two between all data sets. The agreement is encouraging in view of the somewhat different times and locations at which the data were obtained.

The "average" profile is characterized by two separate gradients which could permit different nomenclature for the region below 70 km and the region between 70 and 85 km. It additionally is characterized by an often seen minimum located close to the mesopause (about 84 km) which tends to separate the D and E regions. The maximum value of  $N_e$  in the D region ( $N_mD$ ) for the stated conditions averages  $700 \text{ electrons cm}^{-3}$ .

A note of caution needs to be injected in the discussion of this average D region profile. The data on which it is based were obtained at what

\*See D Region Chapter.

event\* (curve C of Figure 1) which is associated with a magnetic disturbance and the precipitation of energetic electrons into the D region. Jackson and Kane (1959) obtained an electron density profile (curve D of Figure 1) during a Polar Cap Absorption\* (PCA) event which is produced by energetic proton precipitation following certain types of solar flares. It should be noted that the PCA data were obtained during the early phases of the event. Ground-based measurements of radio absorption indicate much larger electron density enhancements during the main phase of a PCA.

Knecht (1963) has called attention to a fourth type of anomalously high D region absorption event observed frequently during the winter at temperate geographic latitudes. Electron density increases of up to a factor of ten have been reported in instances not associated with magnetic disturbances or a PCA event. In general, since these and seasonal variations in  $N_e$  have been inferred from ground-based techniques, the  $N_e$  profiles likely should be treated as qualitative because the measured phenomena might also represent temporal changes in the electron collision frequency parameter, which was assumed to be constant in deriving  $N_e$ .

#### 4. AN AVERAGE E REGION ELECTRON DENSITY PROFILE

The altitude interval ascribed here to the E region lies between 85 and 140 km. The largest body of data concerning its behavior has been obtained by use of the conventional ground-based ionosonde. These results are particularly important to our understanding of the geographic and temporal variations of the E region under sunlit conditions. Unfortunately, the ionosonde experiment is not well suited for the determination of the detailed altitude dependence of E region electron densities, especially under nighttime conditions.

Our knowledge of the fine structure of the E region electron density profile has come from rocket experiments. These have been of two general types: radio propagation between the rocket and the earth and direct-sampling probes. It generally is recognized that the propagation experiments produce the most accurate profiles because they are relatively free of possible errors

originating from the disturbance introduced into the medium under study by the rocket carrier. However, quite recently the probe experiments have been "calibrated" by including them on the same rocket flights that contain propagation experiments. This lends confidence to the validity of nighttime electron density profiles discussed in the succeeding section and which have been obtained from probe experiments because of their inherent high sensitivity.

An E region  $N_e$  profile representing the average obtained by many rocket experiments is identi-



FIGURE 2.—D and E region electron density profiles

fied as the upper portion of curve A in Figure 2. It is evident that the E region profile contains two distinct altitude intervals. The first (85–100 km) is characterized by one of the largest positive electron density gradients (about  $10^4$  electrons  $\text{cm}^{-3}$  per kilometer) found in the ionosphere. Most theoreticians ascribe the electrons found in this altitude interval to the combined effects of Lyman  $\beta$  (1026 Å) and x-radiation (100–30 Å).<sup>†</sup> The second region (100–140 km), believed to result from the combined effects of x-rays and of radiation principally in the 1027–911 Å portion of the ultra-violet spectrum,<sup>†</sup> is characterized by a relatively constant electron density. In fact, it is the absence of a significant "valley" in the daytime profiles that represents one of the most important results of the early rocket experiments. This feature has made it quiet difficult to discuss separately the E and F regions of the ionosphere.

<sup>†</sup>See E Region Chapter.

### 5. VARIATIONS FROM THE AVERAGE E REGION ELECTRON DENSITY PROFILE

The major change from the average E region profile is *diurnal* in nature. It is possible from ionosonde data to construct a detailed temporal variation at specific latitudes of the maximum electron concentration ( $N_mE$ ) in the E region for the sunlit hours. There is a symmetrical variation about a noontime value of  $1.2 \times 10^5$  electrons  $\text{cm}^{-3}$  down to  $5 \times 10^4$  electrons  $\text{cm}^{-3}$  near the sunrise and sunset hours. Two nighttime profiles obtained from rocket experiments by L. G. Smith (1962) are presented in Figure 2, curve B representing an evening condition and curve C a pre-dawn situation. With the exception of the much lower value of  $N_mE$ , the features that best distinguish the nighttime profiles from the average profile are (a) the existence of a "pronounced" value above 110 km which extends into the F1 region and (b) the irregular fine structure. Profiles diurnally spaced as in Figure 2 have been used to infer the rate of destruction of electrons in the E region. They are believed to be lost mainly by recombination with diatomic ions.\* An effective E region recombination coefficient of  $2 \times 10^{-8} \text{cm}^3 \text{sec}^{-1}$  has been computed from data such as that contained in Figure 2.

*Solar cycle, seasonal and latitude variations* of  $N_mE$  are small compared to a complete diurnal variation. This conclusion from ionosonde data is quite important since it tends to narrow the hypotheses concerning formation of that portion of the E region lying above 100 km to those which include ionization sources having quite stable long term characteristics. Additionally, there is an important implication in favor of a time independent structure of the neutral atmosphere. Ionosonde data indicate that the noontime value of  $N_mE$  is only about 50 percent larger during sunspot maximum than during sunspot minimum. There are seasonal variations in  $N_mE$  of up to a factor of two at midlatitudes with the maximum occurring in June and the minimum in December in the northern hemisphere.

The perturbations in E region electron density during solar flares, magnetic storms and auroral events are known from ionosonde data to be small

compared to the above-described diurnal, solar cycle and seasonal effects. This most likely is because such events are associated with energetic radiation which penetrates into the D region before ionization results. The most frequent E region anomaly is not necessarily associated with such events. Rather, it exhibits a rather random temporal variation which has led to the nomenclature of sporadic-E or  $E_s$  ionization.

One common form of  $E_s$  ionization is a thin layer in which the electron density is considerably higher than the region immediately below and above. Rocket experiments have best described the altitude characteristics of this type of  $E_s$  ionization, examples of which are illustrated by the dashed portions of the nighttime profiles shown in Figure 2. It is seen that the  $N_s$  enhancement can be as large as 6 and that the thickness of the layer measured at half the peak electron density can be smaller than 0.5 km. Larger  $N_s$  enhancements have been observed and there is evidence that the horizontal extent sometimes is measured in hundreds of kilometers. Another common form of  $E_s$  ionization is characterized by large electron density gradients lying below a region of relatively constant electron density.

Smith (1957) and Seddon (1962) have reviewed the occurrence probability of  $E_s$  ionization. Seddon finds that the preferred altitudes are 100, 105, 111, 117 and 129 km, three of which are approximately confirmed by the nighttime profiles shown in Figure 2. Smith finds that  $E_s$  is principally a nighttime phenomenon in and near the auroral zone but conversely that it is more a permanent daytime feature in a narrow band centered at the geomagnetic equator. Here we caution again that auroral characteristics might extend to magnetic dips as low as  $70^\circ$  and consequently in North America down to what normally is considered mid-latitudes. At the middle magnetic latitudes, the  $E_s$  occurrence probability is mostly seasonal in nature with the predominance in summer months.

There undoubtedly are several causative mechanisms for  $E_s$  phenomena, the most likely being the combined existence of wind shear and magnetic field for the mid-latitudes and two stream plasma instability for the equatorial and perhaps the auroral zones (cf Knecht, 1963).

\*See E Region Chapter.

## 6. AN AVERAGE F REGION ELECTRON DENSITY PROFILE

Of all the ionospheric subdivisions, the F region is the most variable. Diurnal, solar cycle and latitudinal effects can each produce changes of almost an order of magnitude. Additionally, seasonal variations are quite large. Thus, it should not be surprising if the average F region profile presented here is rarely observed.

The average F region profile, constructed from rocket results obtained under the appropriate conditions, is superimposed on the average D and E region profiles as curve A in Figure 3. As

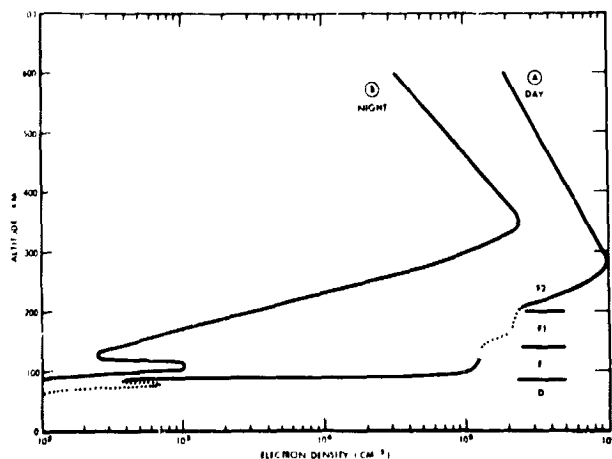


FIGURE 3.—Typical D, E, and F region electron density profiles

shown, the F region contains the altitude ( $h_{\max}F2$ ) of the maximum electron concentration ( $N_{\max}F2$ ) found in the ionosphere. Average values for  $h_{\max}F2$  and  $N_{\max}F2$  are 280 km and  $10^6$  electrons  $\text{cm}^{-3}$ , respectively. The daytime sub-peak region can be divided into two altitude intervals, the bases of which are identified by positive electron density gradients. The classical nomenclature for these subdivisions are F1 (approximately 140–200 km) and F2 (above 200 km).

It is likely that the electrons in the F region are produced by the same portion of the ultra-violet spectrum as for the upper E region. The  $N_e$  gradients that identify the F region probably are the result of changes from electron loss through direct recombination to loss mechanisms involving an intermediate process of ion-atom interchange prior to recombination.

In addition to electron production and loss, a third process (diffusion) becomes effective at higher F2 altitudes and contributes to the formation of the F2 peak. Diffusion or motion of the electron-ion gas can take place in accordance with gravitational or electro-magnetic forces. Diffusion is more effective than electron production or loss at altitudes above the F2 peak and is the reason for the exponential decrease of  $N_e$  with altitude.\*

Our average F2 region can be defined in the Northern Hemisphere as lying between  $40^\circ$  and  $70^\circ$  magnetic dip. This permits us to minimize the corpuscular radiation effects that influence auroral ionosphere and also to neglect diffusion of the thermal electrons horizontally along magnetic field lines, a low latitude phenomenon. In this restricted reference latitude region, the tendency is for the upper ionospheric electrons to be distributed in accordance with diffusive equilibrium. Specifically, the profile above  $h_{\max}F2$  is heavily dependent on the mean ionic mass and the average of the electron and ion temperatures. The reference upper ionosphere profile in Figure 3 is characteristic of that obtained in the presence of a single ionic constituent ( $O^+$ ) and an average isothermal electron-ion temperature of  $1600^\circ\text{K}$ .

## 7. VARIATIONS FROM THE AVERAGE F REGION ELECTRON DENSITY PROFILE

The existence of a distinct F1 region is only a daytime feature of the ionosphere. Furthermore, there is ionosonde evidence that even its very existence under daytime conditions is seasonally dependent. Its occurrence probability is highest in summer at solar maximum and is extremely low in winter at solar minimum. When it does exist, the maximum electron density values ( $N_{\max}F1$ ) show only a small dependence on temporal position within a solar cycle.

The behavior of  $N_{\max}F2$  and of  $h_{\max}F2$  is extremely complicated. At mid-latitudes, during winter months,  $N_{\max}F2$  decreases by a factor of about 4 from day to night. This diurnal effect is accompanied by an increase in  $h_{\max}F2$  of about 70 km. These features are brought out in Figure 3 by comparison of curves A and B which respectively represent day and night conditions. It

\*See F Region Chapter.

should be noted that at night the breadth of the F2 peak is smaller and more importantly, that above the F2 peak there is a more rapid decrease of  $N_e$  with altitude. The more rapid decrease is brought about by a corresponding reduction of the electron and ion temperatures.

It is known from ionosonde data that, at mid-latitudes in winter, there is up to an order of magnitude decrease in  $N_{max}$  from solar maximum to solar minimum. The solar cycle effect is smaller in summer than in winter. To illustrate further the extreme variability of the F region we are faced with a seasonal anomaly, wherein for a given epoch there is a decrease in  $N_{max}$  of up to a factor of four from winter to summer.

Because it only has been recently explored to any extent, detailed temporal variations of the upper F region consist only of diurnal studies based principally on Alouette Topside Sounder Satellite results. Observational Alouette data (Bauer and Blumle, 1964) illustrating the diurnal variation of  $N_e$  for altitudes between 400 and 1000 km are shown in Figure 4. They are applicable

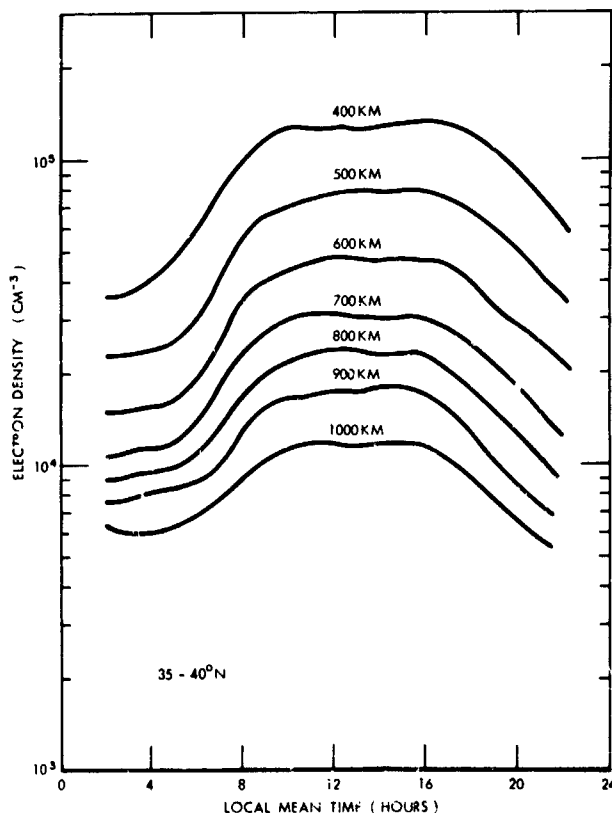


FIGURE 4.—Diurnal variation of electron density in the upper ionosphere (Bauer and Blumle, 1964)

to October-December, 1962, and thus are more representative of solar minimum conditions. The data apply only to geographic latitudes 35–40°N over North America which lie within our definition for average F2 conditions. The most striking feature is that the diurnal variation decreases with altitude. This may be caused by the relative importance of the  $O^+$ ,  $He^+$ ,  $H^+$  ions which vary between night and day in such a way that the lighter constituents become more important at night. The lower mean ionic mass at night tends to overcome the effect of lower charged particle temperatures and lower values of  $N_{max}$  in determining the electron density at higher altitudes.

As we have implied previously, there is a pronounced latitude effect on the F2 region. The existence of an ionospheric equatorial anomaly was first detected by ionosonde experiments which since have provided details of its bottomside characteristics. A more detailed description of the anomaly has come from the dramatic results of the Alouette Topside Sounder Satellite. An idealized representation of the diurnal behavior of this anomaly over South America is illustrated in Figure 5 (Jackson, 1964). It was prepared by combining the satellite results of Lockwood and Nelms (1964) with ionosonde data by Wright (1962). Plotted are idealized isoelectronic contours as a function of altitude and latitude for

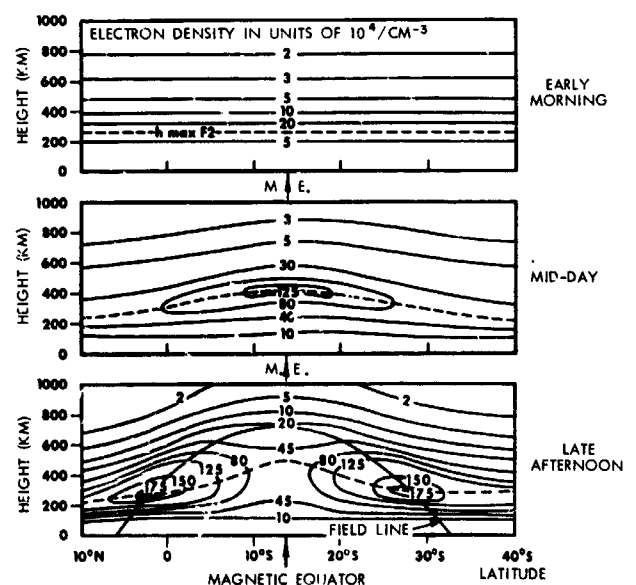


FIGURE 5.—Idealized representation of the equatorial anomaly (Jackson, 1964)

three diurnal conditions representative of the late 1962 period.

It is seen from Figure 5 that the anomaly is mainly a daytime feature. For midday conditions, a pronounced dome or peak in electron density occurs over the geomagnetic equator with a corresponding increase in  $h_{\max}F2$ . In late afternoon, the equatorial dome is the dominant feature only at altitudes above 600 km. Below this altitude, two  $N_e$  peaks are located symmetrically about the geomagnetic equator along a specific magnetic field line. King et al (1963) have made satellite studies of the anomaly near Singapore with somewhat different results. They find that the formation of the double peak occurs much earlier in the day for the easterly longitudes. The diurnal behavior of the equatorial anomaly suggests that its characteristics are closely related to the competition between electron production which tends to maximize  $N_e$  at the sub-solar latitudes and diffusion along magnetic field lines which tends to produce a symmetrical  $N_e$  distribution about the geomagnetic equator.

The equatorial anomaly causes the appearance of small ionization ledges to appear on  $N_e$  altitude profiles wherever the appropriate magnetic shell appears. The appropriate shell for this case using the McIlwain (1961) notation occurs at magnetic L values which vary from 1.06 to 1.18. This particular field-aligned ionization enhancement has been verified experimentally by direct measurements of  $N_e$  on the Ariel satellite (Sayers et al, 1963) and by Alouette satellite results (King et al, 1963). The latter have identified additional field-aligned ledges detected from the Ariel and/or Alouette satellite results with the region of maximum flux of electrons from the artificial radiation belt ( $L = 1.22 \pm .02$ ), with the heart of the inner radiation belt ( $L = 1.6 \pm 0.1$ ) and with the most intense portion of the outer radiation belt ( $L \cong 4.0$ ). Other ledges appear at  $L = 2.2 \pm 0.1$  and at  $4.5 < L < 6.5$ .

At higher latitudes, the electron scale height at 500 km increases markedly with latitude from what would be inferred from Figure 4 (King et al, 1963). There also is evidence (Bauer and Blumle, private communication) that at the higher latitudes the diurnal variation of  $N_e$  above  $h_{\max}F2$  is relatively constant with altitude, in contrast

with the middle latitude results represented by Figure 4.

### 8. ELECTRON DENSITIES AT VERY HIGH ALTITUDES

Very few electron density distributions have been obtained for the region above 1000 km at magnetic dips  $40^\circ$ – $70^\circ$ . The few that do exist (cf Hanson, 1962; Bauer and Jackson, 1963; Donley, 1963) have been interpreted in terms of an isothermal ionosphere in diffusive equilibrium.

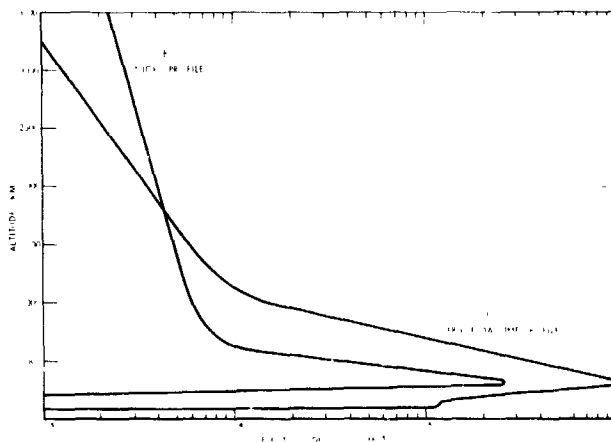


FIGURE 6.—Electron density profiles in the outer ionosphere at mid-latitudes

In Figure 6, two such profiles, one for a daytime (curve A) and the other for a nighttime conditions (curve B) have been superimposed on a typical lower ionosphere profile. The distribution above 1500 km for the daytime case corresponds to what would be expected for a plasma predominated by  $He^+$  ions and for an average electron-ion temperature of  $1600^\circ K$ . This infers that protons for the daytime ionosphere in the middle of the solar cycle do not become effective below 3500 km (cf Hanson, 1962). The distribution above 1000 km for the nighttime case, on the other hand, corresponds to  $H^+$  ions and an average electron-ion temperature of  $800^\circ K$ . The two profiles suggest that electrons are more abundant at the very high altitudes for a nighttime than for a daytime condition. It should be remembered, however, that the available rocket data on which these profiles depend were obtained at different portions of the solar cycle. Still, it is also possible to infer greater electron densities at night at altitudes above 1500 km by extrapolating profiles

constructed from the diurnal F region variations of Figure 4. This conclusion does not necessarily apply at other than mid-latitudes.

More extensive observations of magnetospheric electron densities have resulted from whistler observations. Carpenter (1963) has summarized the whistler measurements of magnetospheric electron densities for equatorial latitudes. His "smoothed" curve is presented in Figure 7.

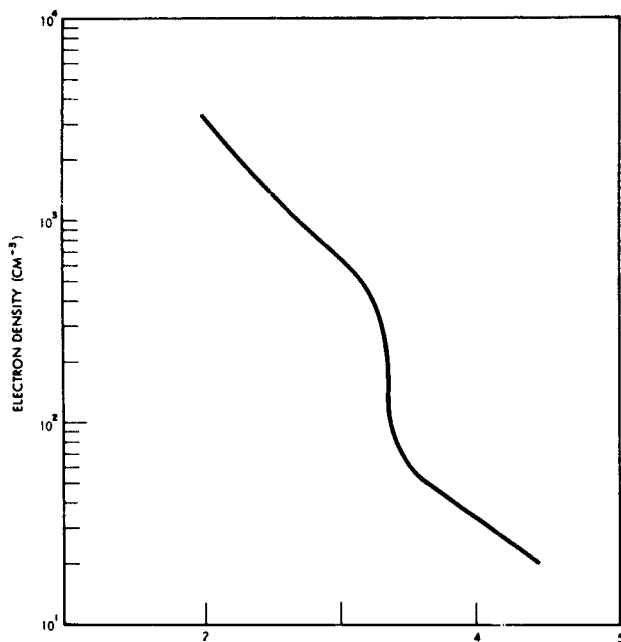


FIGURE 7.—Equatorial profile of magnetospheric electron density (Carpenter, 1963)

The most pronounced characteristic is the knee located at about  $3R_E$  where the density drops by a factor of 6 or more. Carpenter finds these results to be consistent with the above-described rocket results, with the USSR results from the Lunik II spacecraft (Gringauz et al, 1960), and with the ground-based incoherent backscatter results of Bowles (1962). He suggests that the position of the "knee" is quite variable, moving from  $2R_E$  during high magnetic activity to  $7-8R_E$  during low magnetic activity. One important implication from Figure 7 is that if one defines the ionosphere as a region containing a significant number of very low energy electrons, then the ionosphere extends out to several earth radii.

## 9. ACKNOWLEDGEMENTS

The stimulating discussions with J. E. Jackson of the Goddard Space Flight Center during the preparation of this review is gratefully acknowledged. The author also is grateful to S. J. Bauer and L. Blumle for access to their data prior to publication.

## 10. REFERENCES

1. AIKIN, A. C., J. A. KANE and J. TROIM, Space Research IV, in press, 1963.
2. BARRINGTON, R. E. and E. V. THRANE, J. Atmos. Terr. Phys., 24, 31, 1962.
3. BAUER, S. J. and L. J. BLUMLE, private communication, to be published, 1964.
4. BAUER, S. J. and J. E. JACKSON, J. Geophys. Res., 67, 1675, 1962.
5. BELROSE, J. S., Proc. International Symposia on Ionospheric Sounding, 1961.
6. BELROSE, J. S. and E. CETINER, Nature, 195, 688, 1962.
7. BOWLES, K. L., NBS Report 7633, 1962.
8. CARPENTER, D. L., Proc. of the XIV URSI General Assembly, 1963, in press.
9. DONLEY, J. L., J. Geophys. Res., 68, 2058, 1963.
10. GRINGAUZ, K. I., V. G. KURT, V. I. MOROZ and I. S. SHLOVSKII, Astronomicheskii Zhurnal, 37, 716, 1960.
11. HALL, J. E., Proc. NATO Advanced Study Institute, Skeinkampen, Norway, in press, 1963.
12. HANSON, W. B., J. Geophys. Res., 67, 183, 1962.
13. JACKSON, J. E., NASA Technical Note, 1964, in press.
14. JACKSON, J. E. and J. A. KANE, J. Geophys. Res., 64, 1074, 1959.
15. JESPERSEN, M., O. PETERSEN, J. RYBNER, B. BJELLAND, O. HOLT and B. LANDMARK, Norwegian Space Res. Comm. Rept. No. 3, 1963.
16. KANE, J. A., J. Atmos. Terr. Phys., 23, 338, 1961.
17. KING, J. W., P. A. SMITH, D. ECCLES and H. HELM, DSIR Radio Research Station Report RRS/I.M. 94, 1963.
18. KNECHT, R. W., Proceedings of the XIV URSI General Assembly, 1963, in press.
19. LOCKWOOD, G. E. K. and G. L. NELMS, J. Atmosph. Terr. Phys., 1964, in press.
20. McILWAIN, J. Geophys. Res., 66, 3621, 1961.
21. SAYERS, J., P. ROTHWELL and J. H. WAGER, Nature, 198, 230, 1963.
22. SEDDON, J. C., Ionospheric Sporadic E, Pergamon Press, Oxford, 909, 1962.
23. SMITH, F. K., NBS Circular 582, 1957.
24. SMITH, L. G., Geophys. Corp. of America., Tech. Rept. 62-1-N, 1962.
25. WRIGHT, J. W., NBS Technical Note 138, 1962.



NG 5-32074

## RESEARCH WITHIN THE IONOSPHERE\*

ROBERT E. BOURDEAU

As in the other space sciences, our understanding of the mechanisms which govern the characteristics of the earth's ionosphere has been enriched by the recent, golden opportunities to perform experiments on rockets and satellites which pass through the medium under study. This understanding also has been improved by the use of new and exciting ground-based experiments.

Traditionally, the ionosphere is defined as that portion of the upper atmosphere which contains a significant number of charged particles with thermal energies (tenths of an electron volt or less). Ionospheric charged particles, electrons and ions, result from ionization of the neutral constituents by ultraviolet and X-radiation from the sun and possibly by corpuscular radiation. The electrons are lost by recombination with the positive ions that are simultaneously produced. The loss rate is slow enough that the ionosphere persists throughout the night especially at the higher altitudes. Because of the high electron number density, the ionosphere classically is associated with its effects on radio communication processes.

In addition to the above-described production and loss-mechanisms, gravitational and electromagnetic forces contribute to ionospheric characteristics. The combination of all these factors is such that several regions with unique features are formed. This natural subdivision permits a discussion of the ionosphere to be subdivided. Specifically, as will be done here, it allows for separate discussions of the D (50-85 kilometers), the E (85-140 km) and the F (140-600 km) regions and of the upper ionosphere which extends from 600 km to several earth radii.

The D, E and that portion of the F region which lies below about 300 km were identified and named as a result of research with the classical tool of

ionospheric research, the ground-based ionosonde. With this "low-frequency radar," one measures the time between transmission of a radio signal from the earth to reception of the echo reflected from the ionosphere. The electron density at the point of reflection is proportional to the square of the frequency. Therefore, when this is done as a function of frequency it is possible to obtain electron density as a function of altitude. We have learned much about the temporal and latitudinal behavior of the electron distribution in the lower ionosphere through long term world-wide use of ionosonde apparatus.

It is the purpose of this paper to summarize recent advances in our understanding of the ionosphere with emphasis on those that have come about as a result of the ability to place observatories in the medium under study. This necessarily involves relating the detailed altitude, latitude and temporal variations of all characteristics of the thermal-charged particles to gravitational and electromagnetic forces, to possible ionizing sources, and to the nature of the neutral atmosphere from which the ions and electrons are created.

### THE NEUTRAL ATMOSPHERE

The neutral atmosphere classically is divided into regions in accordance with the variation of temperature with altitude. The altitude dependence of temperature is represented for average daytime conditions<sup>7</sup> in Fig. 1a. Free electrons are found in significant abundance only above 50 km. Consequently, the regions of the neutral atmosphere that are of major interest to the ionosphericist are the mesosphere, which lies between the temperature maximum at 50 km and the minimum near 85 km, and the thermosphere (above 85 km).

\*Published in *Science*, 148 (3670): 585-594, April 30, 1965.

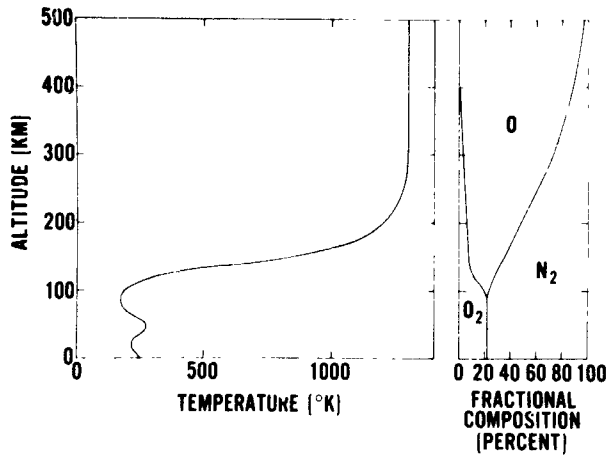
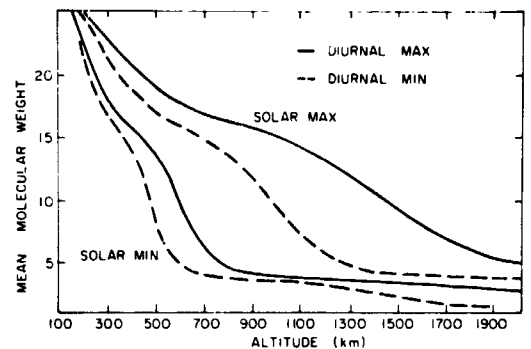


FIGURE 1.—Altitude dependence of neutral gas temperature and fractional composition (Johnson, 1962).

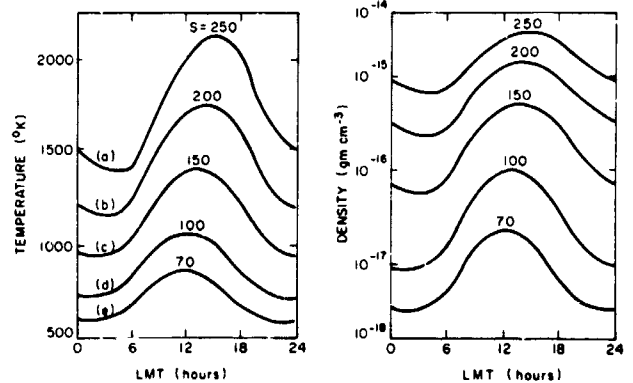
Mesospheric temperatures have been deduced principally from rocket-borne pressure gages and by sound-velocity experiments using rocket-borne grenades. These data show that the mesosphere exhibits large latitudinal and seasonal variations.<sup>1</sup> The large increase of temperature in the lower thermosphere is due principally to the absorption of solar ultraviolet radiation. Heat conduction keeps the temperature nearly constant above 200 km.<sup>2</sup> Thermospheric temperatures have been deduced mainly from atmospheric density measured by use of gauges flown on rockets<sup>3</sup> and satellites<sup>4,5</sup> and indirectly by studying satellite orbital decay.<sup>6</sup>

From the standpoint of theories of formation of the ionosphere, the most important parameter of the neutral atmosphere is its composition. An average percentage distribution of the major constituents is presented<sup>7</sup> as a function of altitude in Fig. 1b. Below 100 km, mixing controls the relative abundance of the neutral constituents and consequently molecular oxygen and nitrogen predominate. Above this altitude, dissociation of atomic oxygen takes place as a result of the absorption of ultraviolet radiation by  $O_2$ . At the higher altitude mixing becomes unimportant and the constituents are in diffusive equilibrium, each component being distributed independently of the others. The distribution of the constituents can be calculated theoretically from <sup>4,7</sup> hydrostatic equation using an assumed altitude for diffusive separation and assumed atmospheric temperatures.

In Fig. 1b, it is shown that the molecular constituents diminish in importance with increasing altitude so that atomic oxygen dominates the atmosphere at 500 km. Above 500 km, the lighter gases become important. Up until an analysis of atmospheric drag on the ECHO I satellite, it was believed that there is a transition directly from an oxygen to a hydrogen atmosphere. However, this analysis<sup>8</sup> first suggested the existence of an intervening helium layer. The importance of neutral helium at the higher altitudes was first confirmed<sup>5</sup> by mass spectroscopy on the Explorer 17 satellite, some time after ionized helium had been detected from rocket<sup>9</sup> and satellite<sup>10</sup> experiments. The thickness and altitude of the helium region should be a strong function of atmospheric temperature.<sup>11</sup> This is reflected in the graphs (Fig. 2a) of mean molecular weight as a function of altitude for the diurnal



(a)



(b)

(c)

FIGURE 2.—Time-dependent model of neutral gas (a) mean molecular weight, (b) thermospheric temperature, and (c) 600 km density, Harris and Priester (1962).

and solar cycle extremes.<sup>12</sup> The region is believed to be diminishingly thin, for example, at night during the year of minimum solar activity.

The structural behavior of the atmosphere shown in Figs. 1b and 2a has been inferred principally from total density measurements using rocket-borne gages and analyses of satellite drag. Early rocket-borne mass spectrometers<sup>13</sup> qualitatively established that diffusive equilibrium controls the composition at the higher altitudes. However, with the early experiments was associated a high probability of errors due to surface recombination within the instruments. Consequently, it has been only in the last year that quantitatively significant measurements of the  $O/O_2$  and  $O/N_2$  ratios were obtained by direct sampling.<sup>5,14,15</sup>

Satellite drag observations show that the temperature and density of the isothermal region of the thermosphere varies considerably with time of day and with the 11-year solar cycle (Figs. 2b and 2c). The five curves<sup>12</sup> in Figs. 2b and 2c are for different levels of solar activity, an index of which is the 10.7 cm flux (S) measured at the earth's surface. Values for S range from 70 at sunspot minimum to  $250 \times 10^{-22} \text{ w m}^{-2} (\text{cps})^{-1}$  during the year of maximum solar activity.

### THE NORMAL D REGION

The D region, which occupies approximately the same altitude interval as the mesosphere (50–85 km), is the lowest region where a significant number of free electrons are found. Here, the relatively dense atmosphere results in a high frequency of collisions between the electrons and the neutral constituents. Consequently, there is a high probability that electromagnetic energy which has been transferred to the electrons will be lost irretrievably in these collisions. Thus, the D region acts as an absorber of radio waves and from this standpoint is the most important ionospheric subdivision. Yet it is the least studied experimentally, primarily for two reasons: (a) the difficulty of devising experiments which are valid in such a weakly ionized medium and (b) the trend on the part of most ionosphericists to perform the more esoteric satellite experiments in the upper ionosphere.

In this section, we shall discuss only the "normal" D region constraining the conditions

geographically to mid-latitudes and temporally to times free of solar flare effects. It wasn't until quite recently that even a preliminary model for the altitude distribution of electrons in the normal D region has evolved, despite the fact that the region is accessible with relatively inexpensive rockets.

The normal D region abundance is too low to permit study by use of the conventional ground-based ionosondes. However, breakthroughs have been accomplished as a result of the development of more complex ground-based radio propagation experiments.<sup>16,17</sup> However, one common denominator of ground-based methods is that the altitude dependence of electron density ( $N_e$ ) is extracted from the data only by assuming an electron collision frequency ( $\nu$ ) profile since both  $N_e$  and  $\nu$  simultaneously affect the measured radio propagation phenomena. On the other hand a collaborative effort on the part of a team of Goddard and Scandinavian investigators<sup>18,19</sup> has resulted in novel experiments involving transmission of radio signals from the ground to rocket-borne receivers. The in-situ reception featured by these complex experiments permits unique separation of  $N_e$  and  $\nu$  with adequate sensitivities for the low densities found in the normal D region.

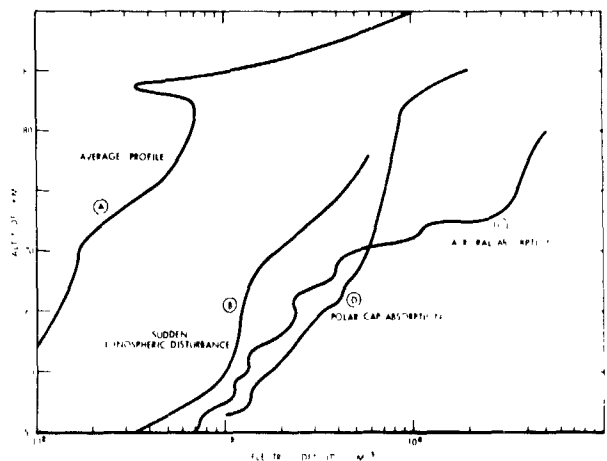


FIGURE 3.—D region electron density profiles.

In Fig. 3, we have combined the few available rocket and ground-based observations to generate an average  $N_e$  profile for the normal daytime D region (Curve A). This profile is only one of the

important pieces of information required to explain how the region is formed. To complete the task requires that one relates  $N_e$  to the competition between electron production and loss for each discrete altitude.

Electron production ( $q$ ) can be computed from a knowledge of (a) the intensity of the ionizing radiation, (b) the density of the ionizable constituents responsive to this radiation and (c) the absorption cross-sections of the ionizable constituents. The problem of estimating  $q$  is complex because the cross-section of each individual constituent is a different function of wavelength if solar radiation is the ionizing source or of electron or proton energy for the case of corpuscular radiation.

In the D region, electron loss is believed to occur mainly through dissociative recombination of electrons with positive ions leading to an excited but neutral constituent. To estimate electron loss requires a knowledge of the recombination rates which are different for each ion species.

As a result mainly of rocket measurements of solar radiation, theoretical models<sup>20</sup> narrow the sources of the normal D region to three individual or combined possibilities. It generally is accepted that the lower part (50–70 km) is produced by the action of cosmic rays on the principal neutral constituents ( $O_2$  and  $N_2$ ). If so, this region should show a strong latitude dependence. There is some disagreement as to the relative roles of the remaining two sources in ionizing the upper part of the D region. Here, one possibility involves the ionization of  $O_2$  and  $N_2$  by 2–8 Angstrom X-rays, an extremely variable source with a very low intensity (not exceeding  $10^{-3}$  erg  $cm^{-3}$   $sec^{-1}$  for a flareless sun). The other possibility is Lyman alpha radiation (1216Å), the only ultraviolet source for which there is a favorable cross-section and which by rocket tests has been observed to penetrate into the D region. This stable but intense source measured in a few ergs  $cm^{-3}$   $sec^{-1}$  acts only upon a trace constituent, nitric oxide. Rocket and satellite measurements indicate that the X-ray fluxes at the extremes of the solar cycle vary by more than two orders of magnitude.<sup>21</sup> Therefore, the relative importance of X-rays and Lyman alpha radiation to the formation of the normal D region may depend on position in the solar cycle.

There have been few spaceflight input-output experiments where the ionization source and the ionization characteristics have been simultaneously measured. According to some observers<sup>18</sup> who measured  $N_e$  on a rocket simultaneously with Lyman alpha flux, X-radiation can be ruled out as a significant source of the normal D region at least for the minimum of the solar cycle. To be certain of the relative importance of these two sources at all times, we desperately need laboratory investigations which can resolve existing uncertainties in our knowledge of the absorption cross-sections and recombination rates.

An important tool in ionospheric research is the ion spectrometer, a very difficult experiment to carry out in the D region—so difficult that it has been carried out only once<sup>22</sup> and this during the last year. Other than possible contaminants borne aloft by the rocket, the major ionic constituent observed below 83 km was  $NO^+$ . This observation supports the Lyman alpha hypothesis but does not rule out, a priori, ionization by X-radiation because of the possibility of ion-molecule interaction.<sup>23</sup> For example,  $O_2^+$  produced directly by X-rays can react with an  $N_2$  molecule to form an  $NO^+$  ion and an NO molecule. Thus, until the various reaction rates are better known, the ion spectrometer observation does not permit a choice between the Lyman alpha or the X-ray hypothesis.

#### SPECIAL D REGION EVENTS

There are many phenomena which can enhance the D region electron abundance by up to more than two orders of magnitude with associated electromagnetic wave attenuation strong enough to produce radio blackouts. Simultaneously with the appearance of a solar flare, increased absorption is observed in the D region on the sunlit side of the earth for periods lasting up to approximately one hour. The causative mechanisms for these sudden ionospheric disturbances (S.I.D.) were not established until investigators accurately timed rocket launchings during the course of a flare and observed enhanced X-ray activity penetrating as low as 30 km.<sup>24</sup> The dominant role of solar X-rays in the production of S.I.D.'s has been confirmed by correlating visible flares with satellite observations of enhanced X-ray fluxes and with increased radio absorption.<sup>21</sup> An order of

magnitude increase in D region ionization during an S.I.D. has been measured with ground-based techniques<sup>16</sup> (Curve B of Fig. 3) and estimated theoretically.<sup>20</sup>

At high latitudes, enhanced radio absorption occurs during auroras. This is attributable to enhanced ionization resulting from direct and indirect (bremsstrahlung) effects of precipitating energetic electrons.<sup>23</sup> Evidence for up to a two order of magnitude increase in electron density has been obtained<sup>19</sup> by timing rocket flights to occur during such auroral absorption events (Curve C of Fig. 3). Another type of absorption takes place above the auroral zone and has been correlated with satellite measurements<sup>25</sup> of enhanced energetic proton fluxes during certain types of solar flares. There has been one rocket measurement<sup>26</sup> of enhanced electron densities during such polar cap absorption events (Curve D of Fig. 3).

Increased radio absorption associated with solar flares is often observed in the winter at middle latitudes. The causes of these events are uncertain. It has been suggested from ground-based observations<sup>16</sup> that these are associated with increases in electron density. However, absorption may also be associated with changes in electron collision frequency. Significant changes in  $\nu$  have been correlated with measured pressure variations in the stratosphere as a result of two rocket flights during which the measured electron densities were approximately the same, thus suggesting a meteorological influence on the D region.<sup>18</sup>

**THE E REGION**

Although ground-based ionosondes have been valuable in detailing the temporal and latitudinal variations of the maximum amount of ionization found in the E and F regions, the important altitude variation of  $N_e$  has come about as a result of rocket probing using both radio propagation<sup>27,28</sup> and plasma probe experiments.<sup>29,30</sup> Typical day and night  $N_e$  profiles composed from such measurements are presented in Fig. 4. These show that at night the D region essentially disappears, the E region electron abundance has decreased by a hundredfold but that there is a strong persistence of the upper F region.

In addition to  $N_e$  measurements, significant contributions to our understanding of the physics

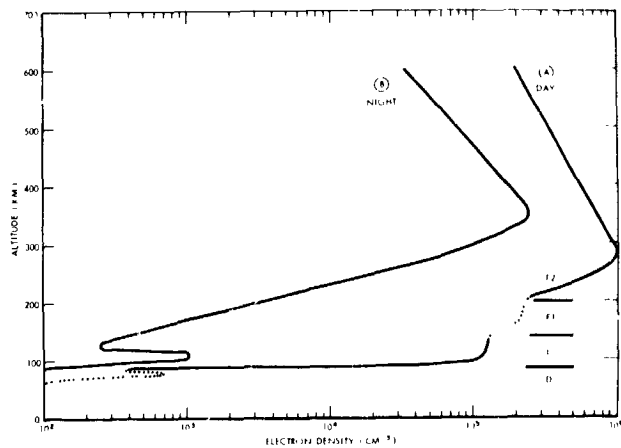


FIGURE 4.—Typical D, E, and F region electron density profiles.

of the ionosphere have come about as a result of vertical cross-sections taken of the intensity of solar radiation<sup>31</sup> and of ionic composition.<sup>32,33</sup> In an important work,<sup>31</sup> solar radiation measurements have been used together with a model neutral atmosphere to estimate the altitude dependence of (a) electron production rate for discrete portions of the X-ray and ultraviolet spectra (Fig. 5a) and (b) the rate of production of each of the

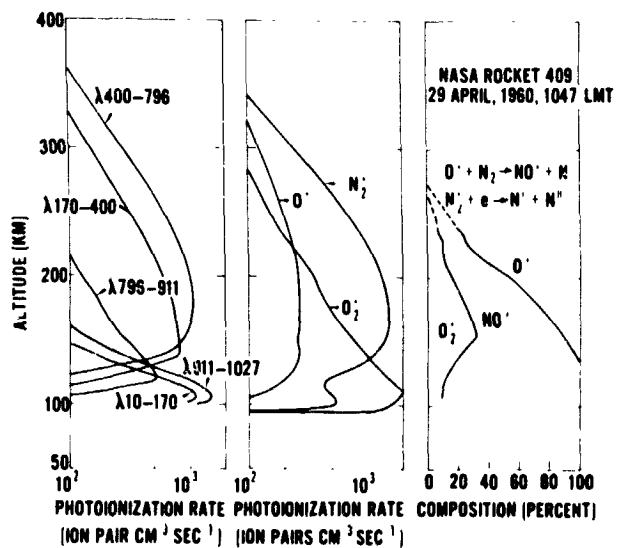


FIGURE 5.—Comparison of ion production rates (Watanabe and Hinteregger, 1962) with rocket measurement of ionic composition (Taylor and Brinton, 1961)

ion species (Fig. 5b). We see that the ions formed at the highest rate are  $O_2^+$ ,  $N_2^+$  and  $O^+$ . Spectrometer observations<sup>32</sup> typically represented in Fig. 5c, on the other hand, show that  $N_2^+$  is a

minor ionic constituent despite the predicted high production rate. They also show that  $NO^+$  is a dominant E region constituent even though it is not significantly produced by direct ionization. Most models<sup>34</sup> attribute the loss of  $N_2^+$  to the combined effects of dissociative recombination with electrons and of ion-atom interchange ( $N_2^+ + O \rightarrow NO^+ + N$ ). The existence of  $NO^+$  generally is explained by ion-atom interchange involving  $N_2^+$  and  $O^+$ .

It should be apparent that our understanding of the formation of the daytime E region has been vastly improved by the above described rocket measurements. Yet, models do disagree considerably as to even the relative importance of X-ray and ultraviolet radiation in the E region. Laboratory measurements of the various rate coefficients and additional rocket flights are needed to resolve these differences.

It wasn't until quite recently that rocket experiments were made sensitive enough for extensive studies of the nighttime E region. In Fig. 4, it is shown that  $N_e$  drops below  $10^3 \text{ cm}^{-3}$  and that the region is characterized by a ledge at about 100–110 km with a valley of ionization just above. It is suggested<sup>33</sup> by a comparison of the results from ion spectrometers flown both during the day and for the first time at night that the maintenance of the nighttime E region is explained by slow decay through dissociative recombination without resort to a nighttime source of ionization. There also is experimental evidence from rockets for metallic ions of meteoric origin in the 100–110 km region.

A frequent anomaly of the E region is sporadic E or  $E_s$  ionization. One common form of  $E_s$  is a layer as thin as 0.5 km in which  $N_e$  is considerably higher than the region immediately below and above, leading to reflection of radio signals at (Fig. 6) abnormally high frequencies. These layers exist at preferred altitudes<sup>35</sup> in the region 100–120 km. Some theories<sup>36</sup> explain  $E_s$  ionization as the result of the combined effects of wind shear and electromagnetic forces. A correlation has been found between wind shear measured on one rocket carrying a sodium vapor release experiment and  $E_s$  ionization detected on a second rocket launched almost simultaneously.<sup>29</sup> However, the exact relationship between  $E_s$  ionization and wind shear is not clear at this time.

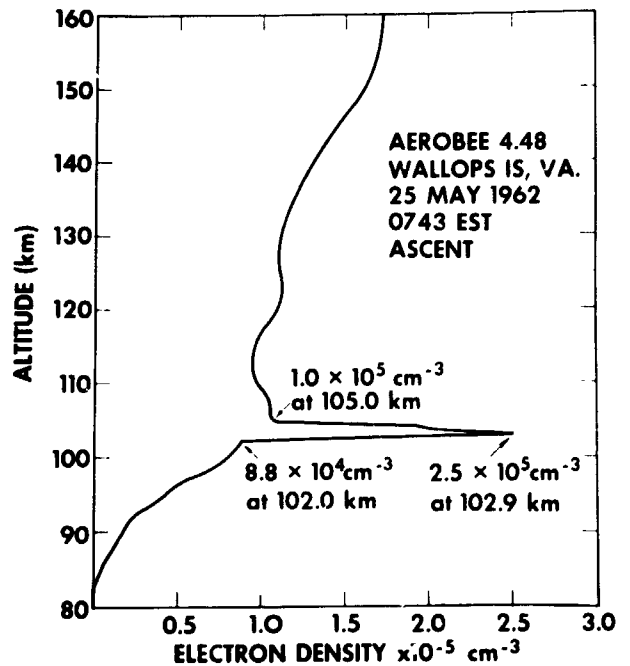


FIGURE 6.—Rocket detection of sporadic-E layer (Smith, 1962).

### THE F REGION

As shown in Fig. 4, the F region contains the altitude of maximum electron density ( $N_m$ ). The region is subdivided into the F1 and F2 regions because a ledge often appears in the daytime 140–200 km region.

It is important to note by comparing Figs. 4 and 5a that the altitude of maximum electron density lies well above the height of maximum electron production. These rocket results confirm previously established theoretical models which ascribe the formation of the F2 peak to charge transport mechanisms of importance comparable to photochemical processes. Specifically, these models ascribe the F2 peak formation to the competition between electron production, a height dependent decrease in electron loss rate and charge transport.

The rocket solar radiation and ion composition measurements (see Fig. 5) show that the origin of F region electrons lies principally in the production of  $O^+$  ions by solar ultraviolet radiation. The dominant F region loss process is believed to be radiative recombination, a two-step process involving firstly ion-atom interchange between  $O^+$  ions and  $N_2$  molecules and secondly recombination of the resulting  $NO^+$  ions with electrons. The slowness of this two-step process is a partial

explanation for the strong persistence of the nighttime F region. The possibility that the electron loss rate decreases more rapidly with altitude than the production rate is an explanation for the experimental observations that  $N_{max}$  lies above the altitude of maximum production.

Because photochemical, gravitational and electromagnetic forces all are effective, the behavior of the F region is extremely complicated. Ionosonde data taken over the last three decades show that the diurnal seasonal, solar cycle and latitude effects each produce large variations in the magnitude and altitude of  $N_m$ .<sup>34</sup> These observations have been related to time-dependent neutral atmospheres deduced from satellite drag measurements (Fig. 2) to estimate ionization, loss and diffusion rates.<sup>37,38</sup>

As the density of the neutral constituents decrease, the importance of photochemical processes diminish. Thus, charge transport processes become dominant and bring about the observed decrease of  $N_e$  with altitude. Gravitational forces, for example, act upon the ions which, by coulomb attraction, cause the electrons to diffuse downward. In this case, the hydrostatic law can be invoked and the electron distribution is controlled by the average electron-ion temperature and the type of ion.

Before rockets and satellites penetrated the upper ionosphere, it was believed that a transition takes place from  $O^+$  ions directly into the protonosphere. However, rocket<sup>9</sup> and satellite<sup>10</sup> experiments indicated that a region of helium ions separated these regions in the daytime during the middle of the solar cycle. Subsequent rocket results<sup>39</sup> suggest that the helium ion region disappears at night. It had been predicted<sup>11</sup> on the basis of the different behavior of the escape rates of hydrogen and helium that both the altitude and thickness of the helium ion region would diminish with decreasing temperature, implying a strong latitudinal and solar cycle dependency.

The role of charged particle temperatures and of ionic composition in controlling the ionosphere is illustrated by rocket measurements of charged particle density taken out to very high altitudes and presented in Fig. 7. Both a daytime and a nighttime result are illustrated. The exponential portions of both profiles provide evidence for a constant electron-ion temperature throughout

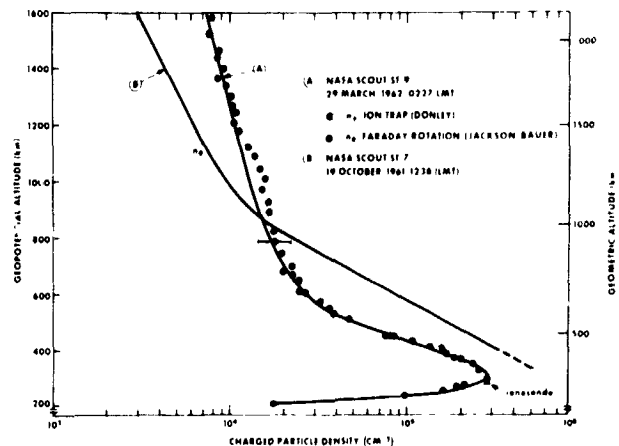


FIGURE 7.—Daytime (Bauer and Jackson, 1962) and nighttime (Donley, 1963) measurements of electron density.

the region with values of  $1300^{\circ}$  and  $800^{\circ}$ K, respectively. The change of slope in both cases is interpreted as the result of a transition from  $O^+$  to lighter ions,  $He^+$  being dominant above this transition for the daytime case but  $H^+$  dominant at night. It is seen that the lower altitude of the transition and the relatively high importance of  $H^+$  causes the surprising result that at very high altitudes the nighttime densities exceed those measured in the daytime. This may not be representative of a true diurnal variation because the two sets of data were obtained in different days.

### SATELLITE STUDIES

Three different types of satellites have been used for ionospheric research each performing a different task. With Direct Measurements Satellites, one uses environmental sampling techniques to measure many ionospheric parameters, but only in the immediate vicinity of the spacecraft. The US Satellite EXPLORER VIII and the British Satellite ARIEL I each contained three major experiments for such studies. The first of these measures electron temperature by techniques similar to those developed by Langmuir in his laboratory studies of gaseous discharges. The second measures the local electron density by use of the radio-frequency impedance characteristic of a probe immersed in the medium. The third type of experiment involves the use of gridded ion traps whose principle of operation is similar to that flown on SPUTNIK III. Here, the high satellite-to-ion velocity permits the trap to act as

a poor man's ion spectrometer such that both ion composition and temperature are obtained.<sup>10</sup>

The second category of satellite (topside sounding) involves the ingenious use of an orbiting ionosonde. As with the classical tool of ground-based ionospheric research, one measures the time between transmission of a radio signal to reception of the reflected echo. For the satellite case the reflection is from the topside of the ionosphere. By sweeping the transmitted frequency, an electron density profile for the region between the F2 maximum and the satellite altitude is measured continuously along the satellite's path. Soundings of the upper ionospheric regions have been made in a near polar orbit for two years with the Canadian Satellite ALOUETTE I, which features a swept-frequency sounder. With a swept-frequency device, one obtains good altitude resolution. The recently-launched US EXPLORER XX features fixed-frequency sounding where vertical resolution is sacrificed so as to better study horizontal irregularities.

The third type of satellite observation involves the study at the earth's surface of the arrival characteristics of radio signals transmitted from the spacecraft at frequencies which penetrate the ionosphere. Faraday rotation and doppler phenomena permit the measurement of the total electron content in a cross-section between the satellite and the receiving site. The first satellite exclusively devoted to this method is Explorer XXII, launched too recently for results to be reported here.

### SATELLITE RESULTS

The major results that have come from satellite studies lie in the unique observations of the latitudinal and diurnal behavior of the regions above the F2 peak and of magnetic-field aligned irregularities.

Evidence for magnetic field control of ionospheric electron densities first came about from the use of ground-based ionosondes, which since have provided details of the bottomside characteristics of the now familiar equatorial anomaly. The morphology of this anomaly has now been obtained to altitudes of about 1000 km. In Fig. 8 are presented results<sup>41</sup> from the Alouette satellite of electron density as a function of magnetic

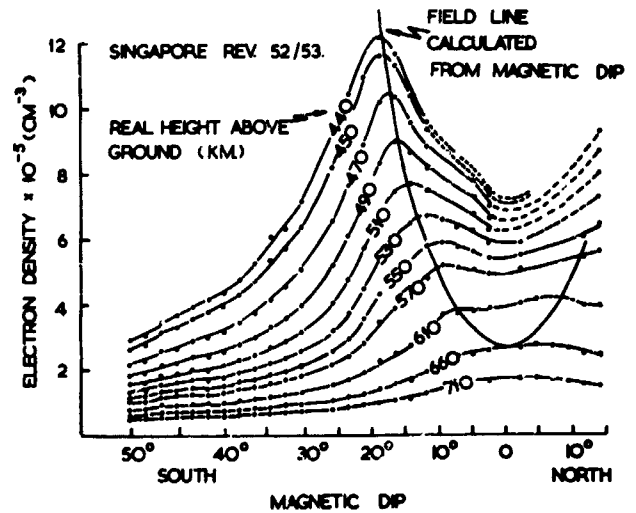


FIGURE 8.—Contours of electron density at constant altitudes measured above Singapore at 1000 LMT (King et al, 1963).

dip for discrete altitudes. These results specifically are for the eastern hemisphere at 1000 local time. A general increase of electron density in the equatorial regions results from diffusion along the nearly horizontal magnetic field lines. For the particular time of day illustrated, the electron density reaches a maximum at the geomagnetic equator for altitudes above about 600 km. Below this altitude, two peaks are symmetrically located along a specific field line. The equatorial anomaly is predominantly a daytime feature of the ionosphere. The altitude above which only a single peak is formed has been termed the "dome" of the anomaly. The altitude of the dome over Singapore varies from 600 km in the early morning and evening hours to a mid-afternoon maximum of about 1000 km.<sup>41</sup> Similar measurements<sup>42</sup> suggest that the anomaly builds up later in the day along the 75th West Meridian. The diurnal behavior of the equatorial anomaly suggests that its characteristics are closely related to the competition between electron production which tends to maximize  $N_e$  at the subsolar point and diffusion along magnetic field lines which tends to produce a symmetrical  $N_e$  distribution about the geomagnetic equator.

Another latitude feature of the topside ionosphere are electron density troughs which appear to be a common phenomenon at middle latitudes during ionospheric storms associated with magnetic disturbances. This is illustrated by Fig. 9,



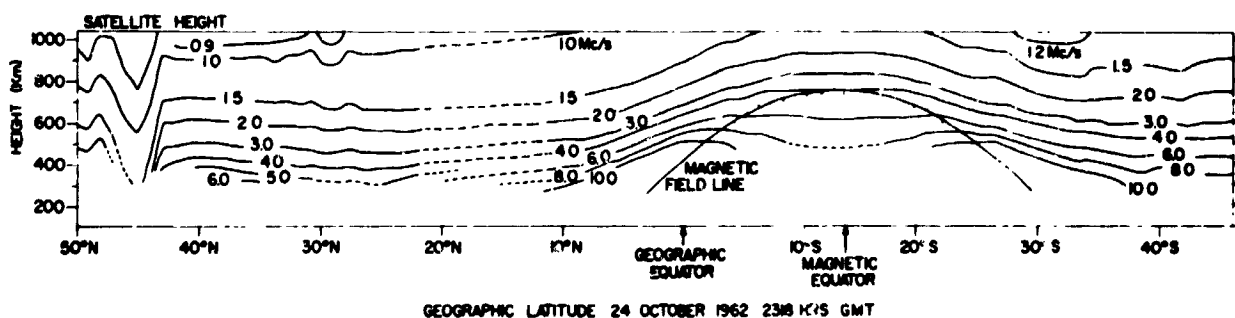


FIGURE 9.—Contours of constant plasma frequency measured with the ALOUETTE satellite (Lockwood and Nelms, 1964)

a plot of Alouette satellite measurements<sup>42</sup> of the frequency of reflections contours. In this illustration, applicable to 65° West Longitude, the trough is less than 5° wide and centered at 45°N.

Evidence for strong magnetic control of the upper ionosphere was first inferred from electron densities measured with an rf probe on the ARIEL satellite.<sup>43</sup> From these observations was inferred the existence of enhanced ionization lying along three specific magnetic field shells, one of which is accounted for by the above-described equatorial anomaly. The existence of these shells of enhanced ionizations were confirmed and others

discovered by the ALOUETTE satellite.<sup>41</sup> Some of these have been associated with the American artificial radiation belt, the heart of the inner radiation belt and near the region of maximum flux of energetic particles in the outer radiation belt. All of these observations suggest that ionization by fast particles should now be considered along with ultraviolet radiation as an ionization source for the F2 region.

A very common anomaly of the F region is the "spread F" condition, where the region shows a diffuse character generally attributed to patches of ionization having concentrations different than

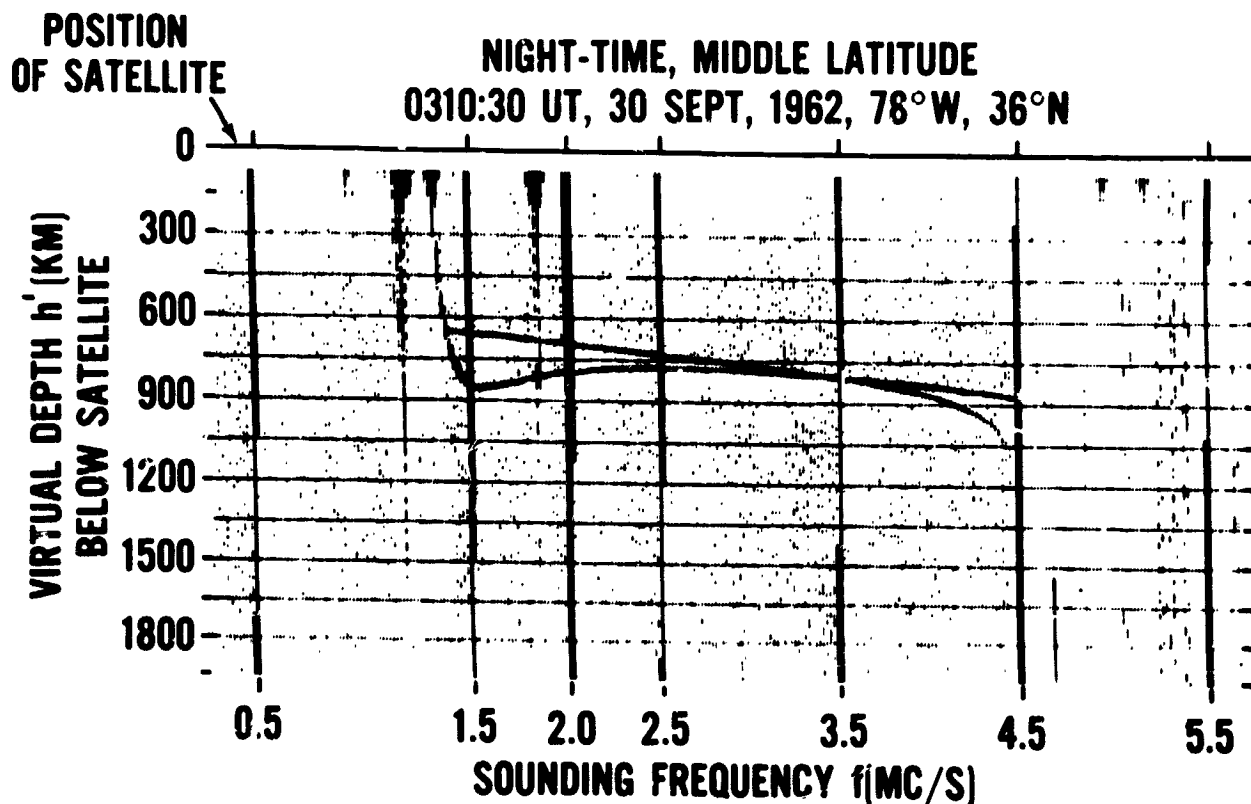


FIGURE 10.—Typical ionogram from ALOUETTE satellite taken in the absence of spread-F.

the immediate surroundings. An ALOUETTE satellite ionogram typical of a homogeneous ionosphere is presented in Fig. 10, the two traces corresponding to the ordinary and extraordinary

electron density is not a strong function of magnetic latitude between about 15 and 45°N geographic latitude. In this region, we can expect that an important charge transport mechanism is

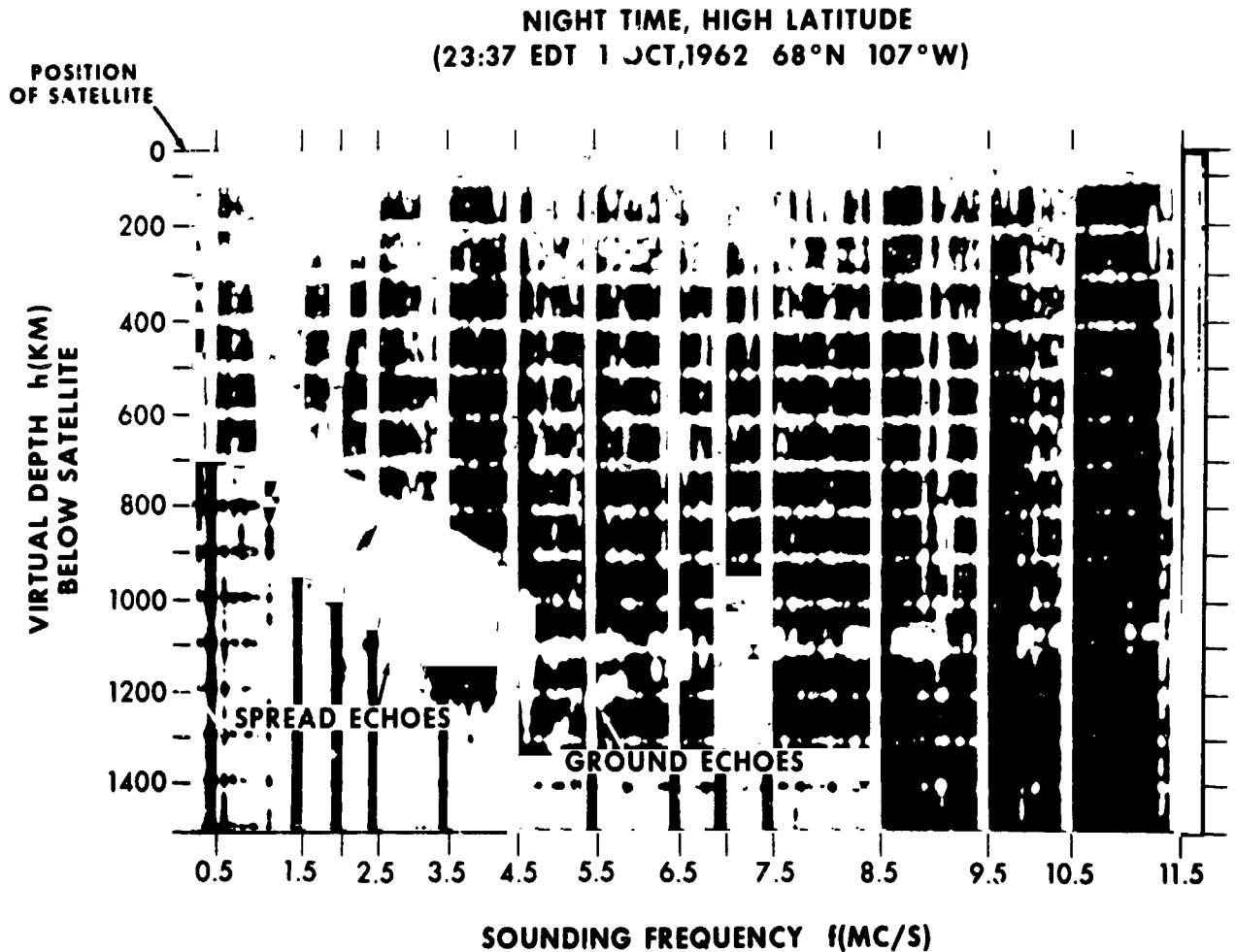


FIGURE 11.—ALOUETTE satellite ionogram taken during the presence of spread-F.

modes of radio-propagation. The effectiveness of spread-F in producing multiple echoes is illustrated by comparing this ionogram with that shown in Fig. 11 which was taken during spread-F conditions. The occurrence probability of spread-F has been the subject of a thorough analysis with the ALOUETTE satellite. This analysis<sup>44</sup> confirms previous ground-based ionosonde studies which showed that the phenomenon is almost a permanent feature of the high latitude ionosphere, occurs only during the night near the equator and that it occurs relatively seldom at mid-latitudes.

Referring back to Fig. 9, we observe that the

due to gravity in which case the electron distribution is a strong function of the mean ionic mass and the average electron-ion temperature. The diurnal variation of the electron distribution in this region has been studied<sup>45</sup> by the use of the ALOUETTE satellite. (Fig. 12). These studies have shown the amplitude of the diurnal variation becomes smaller with increasing altitude. This would confirm a conclusion based on the rocket results shown in Fig. 7 that because of the increased relative importance of the light ionic constituents, the electron densities above 1000 km at night are higher than for a daytime condition. The diurnal variation shown in Fig. 12 have been

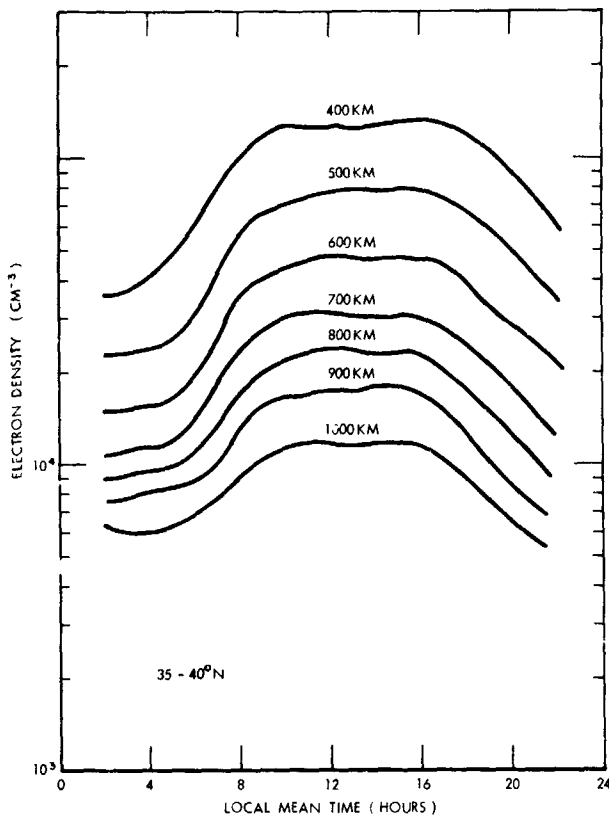


FIGURE 12.—Diurnal variation of electron density in the topside ionosphere (Bauer and Blumle, 1964).

treated in terms of ionic composition and charged particle temperature, one possible result being that for daytime at 500 km the principal ion is  $O^+$  with an average electron-ion temperature of about  $1500^\circ\text{K}$ , while at night the lighter ionic constituents become important even at altitudes as low as 500 km.<sup>45</sup>

#### CHARGED PARTICLE TEMPERATURES IN THE UPPER IONOSPHERE

Because electron ( $T_e$ ) and ion ( $T_i$ ) temperatures are important to the behavior particularly of the region above 300 km, it is important to perform experimental observations of these parameters. Upon their creation, photoelectrons will possess energies in excess of the ambient electrons. They attempt to share this excess energy with the ambient electrons either by direct elastic collisions or after some of the excess energy has been lost through previous inelastic collisions with the ambient neutral particles or positive ions. As a

result, there is a tendency for the ambient electron gas to be hotter than the neutral gas, at least in the daytime. It generally is accepted that at the lower altitudes where the neutral gas density is relatively high, the ion and neutral gas temperatures will be identical. At the higher altitude where the percentage ionization is becoming appreciable, there is a possibility that the ions are in better thermal contact with electrons than with the neutral particles and consequently the ion temperature can be elevated above the neutral gas temperature.<sup>46</sup>

Measurements made with the EXPLORER VIII satellite first indicated a strong diurnal control of ionospheric electron temperatures.<sup>47</sup> Later results with the ARIEL satellite<sup>48</sup> and with ground-based radar incoherent backscatter apparatus<sup>49</sup> confirmed this diurnal dependency. The ARIEL results and a comparison of radar backscatter observations at two locations<sup>49,50</sup> showed that there also is a strong dependency of  $T_e$  upon magnetic latitude. Both the diurnal and latitudinal control of  $T_e$  were subsequently confirmed<sup>5</sup> with the EXPLORER 17 satellite. The observations together show that the daytime ratio of  $T_e$  to the neutral gas temperature can reach values up to 2 depending on latitudinal and temporal conditions.

Since newly-created electrons share their excess energy with the ambient electrons, it follows that  $N_e$  and  $T_e$  should be strongly coupled. The latitudinal behavior of  $T_e$  for the daytime ionosphere thus can be explained in terms of magnetic field control of the electron density at least at moderate altitudes. But, it has been observed that  $T_e$  increases with altitude above 600 km.<sup>48</sup> This would not be expected if direct effects of solar ultraviolet radiation constitute the only source of daytime charged particle heating. The observations<sup>48</sup> are consistent with the hypothesis<sup>46</sup> of possible indirect effects of ultraviolet radiation, specifically a mechanism whereby all of the newly-created electrons do not deposit their energy in the lower F region where they are created but where some are permitted to diffuse along magnetic field lines and deposit the energy at high altitudes. Another important observation<sup>5,48</sup> is that the electron temperature is somewhat higher than the neutral gas temperature at night. This requires a nighttime source of particle heating having an

intensity which is a small fraction<sup>48</sup> of the daytime ultraviolet source.

### THE UPPER IONOSPHERE

In this paper, the higher altitudes have been subdivided into the F region where  $O^+$  ions dominate and the upper ionosphere where light ionic constituents are more abundant. Most observations show that on the average, the transition altitude between these two regions is about 600 km. EXPLORER VIII<sup>51</sup> and ARIEL<sup>52</sup> satellite results show that the transition is from  $O^+$  to  $He^+$  and then to  $H^+$  as the altitude increases, at least during the middle of the solar cycle. These results also show that the thickness and altitude of the helium ion region decrease drastically from day to night. Other results show a more complicated behavior in which for nighttime conditions, and for all diurnal times during the year of minimum solar activity, helium ions are never dominant. The exact morphology of upper ionospheric composition is not yet clear.

It has been suggested<sup>53</sup> that the mean ionic mass is a function of the ion temperature. There already exists evidence<sup>49</sup> that the ion temperature in the upper ionosphere is controlled by the electron temperature which we have shown exhibits a complicated diurnal and latitudinal behavior. It is becoming clear that theoretical models of the F region, the upper ionosphere and the interdependence of these two regions need to be updated to include (a) gravitational forces into which are inserted charged particle temperatures and ionic composition that are temporally and latitudinally variable; (b) the possibility of an ionization source related to fast particles which is superimposed in the ultraviolet source and which contributes to the maintenance of the nighttime ionosphere and (c) the possibility of indirect ionization from ultraviolet radiation, specifically the effect of photoelectrons diffusing from the lower F region along magnetic field lines to deposit their energy at the higher altitudes. Thus although satellite and ground-based studies in recent years have provided a preliminary description of the charged particle parameters at high altitudes, the observations need to be extended and correlated with measurements of photoelectron and fast particle fluxes before adequate theories of formation of these regions can be formulated.

### REFERENCES

1. W. NORDBERG and W. G. STROUD, NASA Technical Note D-703, (1961).
2. L. SPITZER, *Atmospheres of the Earth and Planets*, University of Chicago Press, (1952).
3. R. HOROWITZ, H. E. LA GOW and J. F. GUILIANI, *J. Geophys. Res.*, 64, 2287-2294, (1959).
4. G. S. SHARP, W. B. HANSON and D. D. MCKIBBIN, *J. Geophys. Res.*, 67, 1375, (1962).
5. N. W. SPENCER, G. P. NEWTON, C. A. REBER, L. H. BRACE and R. HOROWITZ, NASA Goddard Space Flight Center Report X-651-64-114, (1964).
6. L. G. JACCHIA, *Planetary Space Sciences*, 12, 355-378, (1964).
7. F. S. JOHNSON, *Astronautics*, 8, 54, (1962).
8. M. NICOLET, *J. Geophys. Res.*, 66, 2263, (1961).
9. W. B. HANSON, *J. Geophys. Res.*, 67, 183-188, (1962).
10. R. E. BOURDEAU, W. C. WHIPPLE, JR., J. L. DONLEY and S. J. BAUER, *J. Geophys. Res.*, 67, 467-475, (1962).
11. S. J. BAUER, *J. Atmos. Sciences*, 19, 276-278, (1962).
12. I. HARRIS and W. PRIESTER, *J. Geophys. Res.*, 67, 4585-4591, (1962).
13. E. B. MEADOWS and J. W. TOWNSEND, *Space Research I*, North-Holland Publishing Co., Amsterdam, (1960).
14. E. J. SCHAEFER, *J. Geophys. Res.*, 68, 1175-1176, (1963).
15. A. O. NIER, J. H. HOFFMAN, C. Y. JOHNSON and J. C. HOLMES, *J. Geophys. Res.*, 69, 979-989, (1964).
16. J. S. BELROSE and E. CETNER, *Nature*, 195, 688, (1962).
17. R. E. BARRINGTON and E. V. THRANE, *J. Atmos. Terr. Phys.*, 24, 32, (1962).
18. A. C. AIKIN, J. A. KANE and J. TROIM, *J. Geophys. Res.*, (November 1964).
19. M. JESPERSEN, O. PETERSEN, J. RYBNER, B. BJELLAND, O. HOLT and B. LANDMARK, *Norwegian Space Res. Comm. Rept. No. 3*, (1963).
20. M. NICOLET and A. C. AIKIN, *J. Geophys. Res.*, 65, 1469, (1960).
21. H. FRIEDMAN, *Astronautics*, 8, 14, (1962).
22. R. S. NARCISI and A. D. BAILEY, *Space Research V*, to be published).
23. A. C. AIKIN, *International Dictionary of Geophysics*, (1964).
24. T. A. CHUBB, H. FRIEDMAN, R. W. KREPLIN and J. E. KUPPERIAN, *J. Geophys. Res.*, 62, 389, (1957).
25. B. MAEHLUM and B. J. O'BRIEN, *J. Geophys. Res.*, 67, (1961).
26. J. E. JACKSON and J. A. KANE, *J. Geophys. Res.*, 64, 1074, (1959).
27. J. C. SEDDON and J. E. JACKSON, *Ann. de Geophys.*, 14, 456, (1958).
28. J. E. JACKSON and S. J. BAUER, *J. Geophys. Res.*, 66, 3055, (1961).
29. L. G. SMITH, *Geophys. Corp. America, Tech. Rept. 62-1-N*, (1962).

30. W. B. HANSON and D. D. MCKIBBIN, *J. Geophys. Res.*, 66, 1667, (1961).
31. K. WATANABE and H. E. HINTEREGGER, *J. Geophys. Res.*, 67, 999, (1962).
32. H. A. TAYLOR and H. C. BRINTON, *J. Geophys. Res.*, 66, 2587, (1961).
33. J. C. HOLMES, C. Y. JOHNSON and J. M. YOUNG, *Space Research V*, (in press).
34. T. E. VAN ZANDT and R. W. KNECHT, *Space Physics*, D. P. GALLEY and A. ROSEN, ed., John Wiley and Sons, New York, (1964).
35. J. C. SEDDON, *Ionospheric Sporadic E*, Pergamon Press, Oxford, 909, (1962).
36. J. D. WHITEHEAD, *J. Atmos. Terr. Phys.*, 20, 49, (1961).
37. H. RISHBETH, *J. Atmos. Terr. Phys.*, 26, 657, (1964).
38. J. S. NISBET and T. P. QUINN, *J. Geophys. Res.*, 68, 1031, (1963).
39. J. L. DONLEY, *J. Geophys. Res.*, 68, 2058, (1963).
40. S. J. BAUER and J. E. JACKSON, *J. Geophys. Res.*, 67, 1675, (1962).
41. KING, J. W., P. A. SMITH, D. ECCLES and H. HELM, *Radio Research Station Report 94*, Bucks, England, (1963).
42. LOCKWOOD, G. E. K. and G. L. NELMS, *J. Atmos. Terr. Phys.*, (1964), in press.
43. SAYERS, J., P. ROTHWELL and J. H. WAGER, *Nature*, 198, 230, (1963).
44. CALVERT, W. and C. W. SCHMID, *J. Geophys. Res.*, 69, 1839-1852 (1964).
45. BAUER, S. J. and L. BLUMLE, *J. Geophys. Res.*, 69, 3613-3618 (1964).
46. HANSON, W. B., *Space Research III*, 282, (1962).
47. SERBU, G. P., R. E. BOURDEAU and J. L. DONLEY, *J. Geophys. Res.*, 66, 4313-4319 (1961).
48. WILLMORE, A. P., *Proceedings of the Royal Society Meeting, May 1963*, in press.
49. EVANS, J. V., *J. Geophys. Res.*, 67, 4914-4920 (1962).
50. BOWLES, K. L., *J. Research NBS*, 65D, 1-14 (1961).
51. BOURDEAU, R. E. and J. L. DONLEY, *Proceedings of Royal Society Conference May 1963*, in press.
52. BOYD, R. L., *Proceedings of the Royal Society Conference, May 1963*, in press.
53. BAUER, S. J., *J. Geophys. Res.*, 69, 553-555 (1964).

# THE TEMPERATURE OF CHARGED PARTICLES IN THE UPPER ATMOSPHERE\*

R. E. BOURDEAU

Three general methods of investigating charged particle temperatures in the upper atmosphere have been used: (a) direct measurements from rockets and satellites; (b) indirect determination using electron scale heights measured from rockets and satellites; (c) ground-based radar incoherent backscatter experiments. The latitude, altitude and temporal trends of these results are reviewed and the implications discussed.

Observations by all three methods are consistent in showing that the electron temperature increases with latitude for both daytime and nighttime conditions. Moderate differences between the daytime electron and neutral gas temperatures are indicated to altitudes well above the F2 peak for a winter mid-latitude ionosphere at an epoch between solar maximum and solar minimum conditions. Much larger daytime differences are observed for summer months and for solar minimum conditions. All of these trends reflect corresponding changes in the electron density.

The daytime observations are consistent with ultraviolet radiation as the predominant heat source if the possibility of photoelectrons diffusing along magnetic field lines and depositing their excess energy elsewhere is included. A nighttime heat source small compared to the daytime ultraviolet effect is required to explain the observations.

## INTRODUCTION

At the first Florence meeting of COSPAR, early direct measurements of electron temperature  $T_e$  were reported from rockets (Aono et al, 1961) and from the Explorer VIII Satellite (Bourdeau, 1961). The Japanese rocket results suggested temperature equilibrium between electrons and neutral constituents in the E region of the daytime ionosphere. Low values of  $T_e$  in the daytime E region subsequently were confirmed by US rocket experiments (Spencer et al, 1962). However, other rocket  $T_e$  measurements (Smith, 1961; Aono et al, 1962; Brace et al, 1963) showed that significant departures from temperature equilibrium are more often observed than not in the E region even at night. The results of Spencer et al (1962) showed that departures from temperature equilibrium extended well into the daytime F region.

Early measurements of charged particle temperatures applicable to the region considerably above the F2 peak at midlatitudes for solar conditions when the 10.7 cm flux index ( $S_{10.7}$ ) was

150  $WM^{-2}CPS^{-1}$  were reviewed by Bauer and Bourdeau (1962) and Bourdeau (1963). Implications of temperature equilibrium at high altitudes which they optimistically derived from the data critically depended on the assumed neutral gas temperature ( $T_0$ ). When these early direct measurements of  $T_e$  and of the average electron temperature  $(T_e + T_i)/2$  obtained from electron density profiles now are compared with more recent reference atmospheres moderate values for  $T_e/T_0$  of about 1.3 are indicated at midday even to altitudes above 1000 km for the indicated level of solar activity. These observations are in approximate agreement with the theoretical model of Hanson (1962) who assumed electron density values close to these particular observational conditions.

More extensive charged particle temperature observations for different epochs of the solar cycle now have been made by use of ground-based radar incoherent backscatter experiments, by additional direct measurements from rockets and satellites and indirectly from electron density profiles obtained from rockets and the Alouette Topside Sounder Satellite. In general, the trend is toward

\*Published as *Goddard Space Flight Center Document X-615-64-103*, May 1964.

much larger departures from temperature equilibrium than indicated in the theoretical models and in the earlier observations especially at the high altitudes.

It is timely then, as is done in this report, to compare these trends with the introduction of latitude and temporal electron density variations in the early theoretical models.

### FACTORS CONTROLLING THE ELECTRON TEMPERATURE

The principal factors controlling  $T_e$  are:

#### Heat Input

1. Solar Ultraviolet Radiation
  - A. Locally-deposited energy
  - B. Diffusing photoelectrons ( $Z > 300$  km)

2. Corpuscular Radiation

#### Heat Loss

1. Inelastic collisions with neutral constituents ( $Z < 250$  km)
2. Elastic collisions with ions ( $Z > 250$  km)
  - A. Ion temperature controlled only by neutral constituents
  - B. Ion temperature also controlled by electrons ( $Z > 600$  km)
3. Coulomb collisions of photoelectrons with ambient electrons

Thermal conductivity in the electron gas ( $Z > 600$  km)

Theoretical charged particle temperature models based on solar ultraviolet heating alone have been developed by Hanson and Johnson (1961), Hanson (1962) and Dalgarno et al (1962). Of these, Hanson's model is the most complete in that he introduced the possibility of (a) photoelectrons diffusing along magnetic field lines and depositing their energy elsewhere, (b) the loss of ion temperature control by the neutral constituents and (c) the importance of thermal conductivity in the electron gas at high altitudes. The indicated altitudes where these factors are important represent Hanson's estimates based on his assumed model atmosphere and electron density profile.

The models of Hanson and of Dalgarno et al each used a single electron density profile and

both depended on rocket measurements of ultraviolet radiation intensity (Hall et al, 1962) to estimate the heat input,  $Q$ . The EUV intensity used applies to a level of solar activity corresponding to  $S_{10.7} \cong 100$ . The heat input is the product of the EUV intensity, the ionization cross-sections and the density of the ionizable constituents and of the heating efficiency. Both theoretical charged particle temperature models exhibit approximately the same altitude behavior wherein low values of  $T_e/T_o$  are indicated in the E region, with the ratio reaching a maximum of about 2.0–2.5 at 200 km and decreasing in the upper F region. A principal and important difference is that the model of Dalgarno et al has  $T_e - T_o$  essentially vanishing above 300 km where Hanson's model permits values for  $T_e/T_o$  of about 1.2 constant at extremely high altitudes.

Because the observational evidence is most heavily weighted for altitudes above the F2 peak, the most important effect to examine is the efficiency of cooling to positive ions. On the assumption that cooling occurs only by elastic collisions to atomic oxygen ions, the electron temperature is given (Hanson, 1962) by:

$$\frac{T_e - T_i}{T_e^{3/2}} \cong \frac{2.1 \times 10^6 Q}{N_e^2} \quad (1)$$

where  $Q$  is the heat input to the electrons expressed in  $\text{ev cm}^{-3} \text{sec}^{-1}$  and  $N_e$  is the electron density. For values of  $Q$  greater than a critical value ( $Q_c$ ) given by

$$Q_c \cong 2 \times 10^{-7} N_e^2 T_i^{-1/2}, \quad (2)$$

there is no solution to (1) and  $T_e$  is not limited by energy transfer to positive ions (Hanson and Johnson, 1961). If  $Q = Q_c$ ,  $T_e > 2T_i$  and if  $Q \gg Q_c$ , very large "runaway" values of  $T_e$  will result and heat conduction in the electron gas is an important effect.

### SOLAR CYCLE VARIATIONS OF $T_e$

In Figure 1 are illustrated daytime mid-latitude electron density profiles typical of December 1960 and 1962, respectively. The principal differences to note are the much higher values of  $N_{\text{max}}$  and  $h_{\text{max}}$  for the 1960 period, and the constant electron scale height for the 1960 case in contrast to the

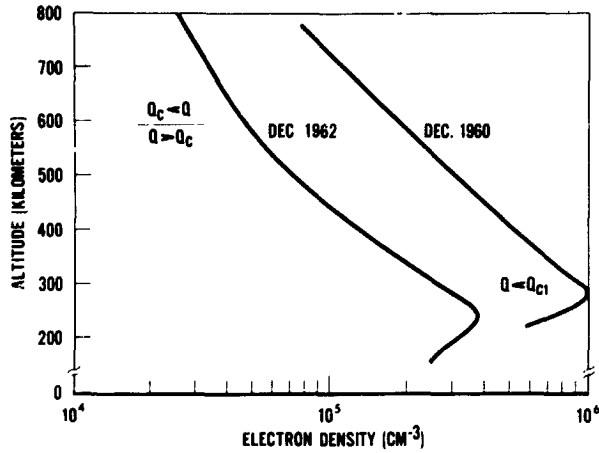


FIGURE 1.—Typical winter mid-latitude electron density profiles.

continually varying scale height for the 1962 profile. The monthly mean of the solar 10.7 cm flux during December 1960 was  $150 \text{ WM}^{-2}\text{CPS}^{-1}$ .

In Figure 2 is presented the mid-latitude diurnal electron temperature variation directly measured

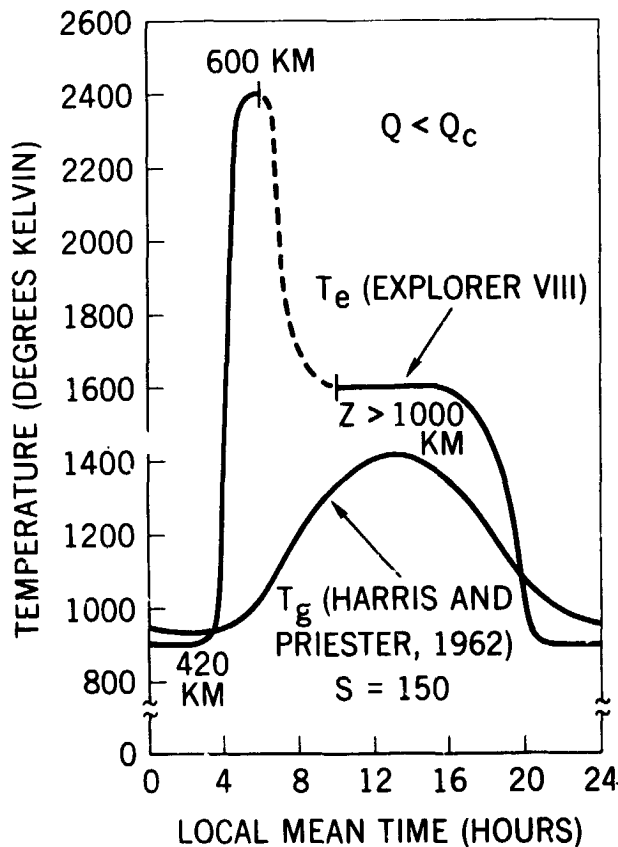


FIGURE 2.—Diurnal electron temperature variation measured during November 1960 from the Explorer VIII satellite for magnetically-quiet days at mid-latitudes assuming  $T_e$  is constant with altitude (425–2400 KM).

during November-December 1960 (Bourdeau and Donley, 1963) from the Explorer VIII Satellite for magnetically-quiet days assuming  $T_e$  is constant with altitude. Depending on which of the current reference atmospheres for the pertinent level of solar activity is used, the average midday  $T_e$  value of  $1600^\circ\text{K}$  taken at midday and at altitudes above 1000 km corresponds to an estimated value for  $T_e/T_g$  of about 1.15–1.33.

It is seen from Equation (1) that the ratio of the heat input to the square of the electron density ( $Q/N_e^2$ ) controls the electron temperature at high altitudes. The value for  $Q/N_e^2$  computed at 400 km from the December 1960  $N_e$  profile in Figure 1 closely corresponds to the value used by Hanson as an upper limit in his model. We have taken into account that the heat input  $Q$  would be larger than in Hanson's case by assuming a linear change of EUV intensity with the decimetric flux index,  $S_{10.7}$ , and a corresponding change in the density of the ionizable constituent,  $n(O)$ . The higher heat input is compensated for largely by the higher electron density than that used by Hanson. Thus we should and do estimate similar values for  $T_e$  as did Hanson. Consequently, we find excellent agreement between the observed  $T_e/T_g$  of 1.15–1.33 and Hanson's theoretical upper limit of about 1.15.

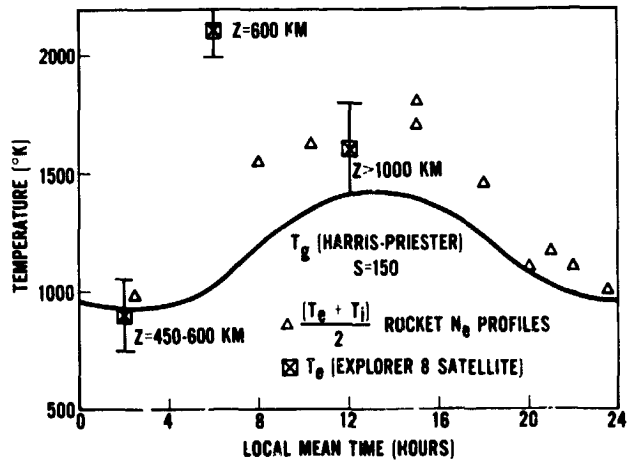


FIGURE 3.—Early charged particle temperature measurements in the upper ionosphere.

In Figure 3, the Explorer VIII data are included with measurements of  $(T_e + T_g)/2$  computed from early rocket  $N_e$  profiles on the assumption of diffusive equilibrium. Of particular



interest is the ion density profile obtained by Hale (1961) at midday and at about the same time as the Explorer VIII observations. Here a value for  $(T_e + T_i)/2$  of  $1600^\circ\text{K}$  (Hanson, 1962b) is derived for the region above 1000 km. The data are too sparse for a firm conclusion but there is a suggestion by the inter-comparison that for winter midday mid-solar cycle conditions  $T_e \cong T_i$  at altitudes above 1000 km but that both the electron and ion temperatures are moderately higher than the neutral gas temperature. This would be consistent with Hanson's arguments that above 600 km (a) thermal conductivity of the electron gas could support differences between  $T_e$  and  $T_i$  which are constant with altitude and furthermore, (b) that the electrons rather than the neutral constituents could control the ion temperature so that  $T_i > T_e$ .

Low midday values of  $T_e/T_0$  at high altitudes also can be implied from the measurement in December 1961 of a value for  $(T_e + T_i)/2$  of  $1235^\circ\text{K}$  (Taylor et al, 1963) from a rocket flight for which an equivalent ion temperature has been inferred (Bauer, 1964). However, we emphasize here Equation (1) and the extreme sensitivity of  $T_e$  to the electron density. We further emphasize that in the actual case, ratios of  $Q/N_e^2$  which permit only moderate rather than large midday departures from temperature equilibrium as is indicated for December 1960 at high altitudes perhaps represent the exception rather than the rule at middle and high latitudes.

Let us consider now the drastic changes in charged particle temperature characteristics as one moves closer to solar minimum conditions. The average value for the index (S) of solar activity corresponding to the December 1962 profile illustrated in Figure 1 was 85. Taking into account a linear decrease in EUV intensity from the time of the rocket EUV measurements (Hall et al, 1962) and a corresponding decrease in the density of the ionizable constituents and computing  $Q_e$  directly from the observed  $N_e$  profile, the estimated ratio  $Q/Q_e$  is larger than 2. Because of the uncertainties in our knowledge of ionization cross-sections and model atmospheres, the computation of  $Q/Q_e$  is suggestive rather than quantitative. Within these uncertainties, it does appear that the EUV effect for low electron densities is sufficient to cause very large electron and

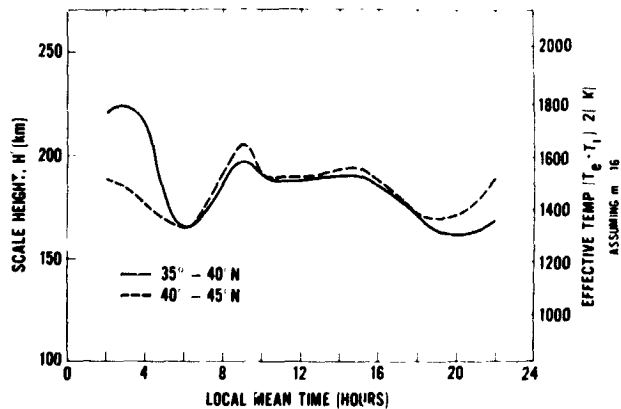


FIGURE 4.—Scale heights at 500 km from ALOUETTE satellite data (Bauer-Blumle, 1964)

possibly runaway electron temperatures.

In Figure 4 is plotted a mid-latitude diurnal variation of electron scale heights calculated for an altitude of 500 km from electron density profiles obtained by the use of the Alouette satellite during the period October-December 1962 (Bauer and Blumle, 1964). It is seen that on the assumption of diffusive equilibrium and  $O^+$  as the principal ionic constituent, values for  $(T_e + T_i)/2$  of  $1500^\circ\text{K}$  are indicated at midday. Assuming  $T_i = T_0$ , a value for  $T_e/T_0$  of about 2.0 is indicated (Bauer and Blumle, 1964), which is much in excess of the December 1960 value. This should not be surprising because of the large increase in the ratio  $Q/N_e^2$  at 400 km and above from December 1960 to December 1962.

If the assumed model atmosphere and ionization cross-sections on which the computation of  $Q/Q_e$  depends are correct, the fact that runaway electron temperatures are not observed suggests that much of the heat input is not deposited locally. Also it should be emphasized that the ratio of 2.0 for  $T_e/T_0$  must be considered an upper limit since it assumes that at 500 km the ion and neutral gas temperatures are the same. Evans (1964) with radar-back-scatter experiments observes at similar latitudes and under similar conditions that  $T_i > T_e$  even as low as 400 km. Thus the values for  $T_e$  implied from Figure 4 may indeed be somewhat overestimated. That the electron temperature begins to control the ion temperature at an altitude lower than that estimated by Hanson is explainable on the basis that the scale heights illustrated in Figure 4 were measured for a different

model atmosphere and electron density profile than that assumed by Hanson.

In summary, the observational evidence as expected shows a large increase in  $T_e/T_0$  between December 1960 and December 1962 which corresponds to a change in the ratio of the heat input to the square of the electron density. In the 1962 case, there still appears to be a sufficient EUV flux to explain the high daytime electron temperatures observed at 500 km during periods of low electron density. There is indirect evidence that some of the energy is not locally deposited and direct evidence from Evans' results that the ion as well as the electron temperature is raised above the neutral gas temperature.

#### SEASONAL VARIATION OF $T_e$

Ionosonde data have shown that the electron density is much higher at the F2 peak in winter than it is in summer. For example,  $N_{\max}$  measured at Washington, D.C., was on the average more than a factor of two larger in the summer than in the winter of 1962. Corresponding changes in  $S_{10.7}$ , which reflect changes in the heat input are not observed. These factors are in the direction of making the ratio  $Q/N_e^2$  much higher in the summer than in the winter months. Consequently, it is possible that, at least for mid-latitudes in the Northern Hemisphere, high ratios of  $T_e/T_0$  will persist high into the upper F region throughout a solar cycle. This could explain why some of the early rocket results taken between solar maximum and solar minimum conditions (cf Spencer et al, 1962) show different electron temperature behavior.

#### DIURNAL VARIATION OF ELECTRON TEMPERATURE

As illustrated in Figure 2, the Explorer VIII satellite results suggest a significant increase in  $T_e$  during the early morning hours. High values of  $T_e$  in the early morning at the F2 peak are also indicated in ground-based backscatter observations (Bowles et al, 1962) and at higher altitudes by Evans (1964).

Early morning maxima in electron temperature have been confirmed by use of the Explorer XVII satellite from which the maximum value of  $T_e$  is placed near 9h local time (Brace et al, 1964).

The electron scale height results from Figure 4 also suggest a maximum  $T_e$  at approximately the same local time (Bauer and Blumle, 1964). Here the high scale heights for nighttime conditions reflect the importance of light ionic constituents. However, for daytime conditions it would be expected that  $m_i$  is relatively constant and thus that the early morning maximum represents a true  $T_e$  maximum. It should be pointed out that the nature and existence of an early morning peak in  $T_e$  has not been emphasized in the Ariel satellite results (Willmore et al, 1963).

It is possible to show from ionosonde data and Equation (1) on the assumption of no EUV absorption above 300 km that the ratio  $Q/N_e^2$  which controls  $T_e$  near the F2 peak maximizes at dawn. However, at high solar zenith angles there could be enough absorption above 300 km to shift the  $T_e$  maximum to later in the morning. This reasoning would insert a latitude and altitude dependence on the time of the diurnal  $T_e$  maximum. It would be expected that the effect becomes more diffuse at higher altitudes because here the diurnal amplitude of the ionizable constituent has increased relative to the amplitude of the diurnal  $N_e$  variation (Bourdeau and Donley, 1963).

#### LATITUDE VARIATION OF ELECTRON TEMPERATURE

Early ionosonde data showed that the daytime electron density at the F2 maximum increases drastically as one goes from mid-latitudes toward the geomagnetic equator. More recently, results from the satellite Alouette has extended the observation that the geomagnetic field plays an important role in governing the electron density distribution to altitudes well above the F2 peak. In Figure 5 is presented an idealized representation of the latitudinal behavior of  $N_e$  prepared by Jackson (private communication) by combining topside sounder (Lockwood and Nelms, 1963) and ionosonde (Wright, 1962) results. Other Alouette data (King et al, 1963) show that the equatorial anomaly builds up earlier in the day at the eastern longitudes. It should be clear from the illustration and Equation (1), that in the daytime  $T_e$  should increase with increasing latitude on the basis of the electron density behavior alone, if we assume no EUV absorption above 300 km and no latitude dependence of the neutral gas character-

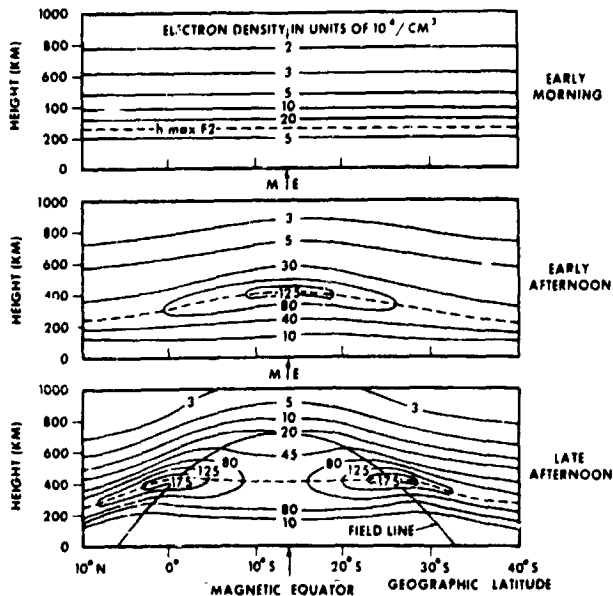


FIGURE 5.—Idealized representation of equatorial anomaly along  $75^\circ$  W meridian based upon data by Lockwood and Nelms (Topside) and J. W. Wright (Bottomside).

istics. An increase of daytime electron temperatures with latitude is indicated by all three methods of charged particle temperature investigation for altitudes below about 800 km. Alouette satellite data suggest constant electron scale heights above 800 km (King et al, 1963).

The ground-based incoherent backscatter results at the geomagnetic equator (Bowles, 1963) show that in the region 200–350 km  $T_e/T_i$  is close to 2 during the daytime hours, maximizing at about 275 km. Above about 400 km in the daytime the results show that  $T_e/T_i$  is unity. Daytime ion temperatures (Bowles, private communication) for March 1964, in the vicinity of  $1000^\circ\text{K}$  are observed. Depending on the adequacy of the Harris-Priester reference atmosphere, this would put an upper limit on  $T_e/T_i$  of 1.2 even during solar minimum conditions. Low values for  $T_e/T_i$  at high altitudes would be expected near the geomagnetic equator because of the generally higher values of  $N_e$  and because near this location diffusion of photoelectrons vertically tends to be inhibited. This supposes heating only by EUV radiation.

The incoherent backscatter results of Evans (1962, 1964) taken near  $50^\circ$  north magnetic latitude show drastically different behavior of charged particle temperatures. This would be expected because of (a) the generally lower value of  $N_e$  than

would exist at the equator, and the higher probability of (b) the photoelectron diffusion effect and (c) additional sources of ionization. The earlier results of Evans' taken in March-April 1962, show daytime ratios of  $T_e/T_i$  of up to 1.6 in the 300–400 km and that  $T_e$  increases with altitude up to 700 km (Evans, 1962). In more recent results taken during July 1963, Evans (1964) offers two possible interpretations for his daytime data obtained for altitudes up to 700 km: (a) if the ionic constituent is all  $\text{O}^+$ ,  $T_e$  and  $T_i$  continually increase with altitude to values of  $2320^\circ\text{K}$  and  $2040^\circ\text{K}$  at approximately 700 km or (b) assuming a mixture of 80 percent  $\text{O}^+$  and 20 percent  $\text{He}^+$  at 700 km,  $T_e$  maximizes at about 450 km then decreases to  $1960^\circ\text{K}$  at 700 km while  $T_i$  increases to a value of  $1410^\circ\text{K}$  at 700 km. The trend of ion composition results (Hanson, 1962; Bourdeau et al, 1962; Bowen et al, 1963; Gringauz et al, 1963; Taylor et al, 1963) would imply that the latter alternative is the more likely. If so, it would be consistent with high values of  $Q/N_e^2$  permitting high values of  $T_e$ , especially below 450 km, and the possibility that cooling to light ionic constituents is becoming effective above 450 km. It should be noted that Equation (1) applies only for  $\text{O}^+$  and that the cooling efficiency to ions should be inversely proportional to the ionic mass,  $m_i$ .

Direct electron temperature measurements measured with the use of the Ariel satellite also show that  $T_e$  significantly increases with latitude (Willmore et al, 1963) the steepest gradient centered at a geomagnetic latitude of about  $20^\circ$ . The midday  $T_e$  value given at the geomagnetic equator for an altitude of 400 km is about  $900^\circ\text{K}$  which compares favorably with  $T_e$  given by Harris-Priester for the pertinent level of solar activity and with the  $T_i$  measurements of Bowles. The trend of the latitude variation at 400 km from the Ariel satellite is generally consistent with the latitude variation  $N_e$  and thus both the ground-based results of Bowles and of Evans (Willmore et al, 1963).

However, the situation above 400 km is more complicated. The Ariel results show  $T_e$  increasing with altitude up to maximum height of the observations at all latitudes. The continuing increase with altitude of  $T_e$  from Ariel at higher latitudes would be consistent with the 1962 results of Evans but not for the likely possibility which Evans offers that  $T_e$  decreases above 450 km for

his 1963 results. We suffer here in the comparison from a lack of simultaneity in the observations. An increase of  $T_e$  at all altitudes in 1962 is perhaps reconcilable with a possible decrease in  $T_e$  above 450 km in 1963 on the base of a lowering with solar activity of the  $O^+ - He^+$  transition altitude.

The fate of the photoelectrons which apparently escape from the altitude of their formation is not yet clear. We have made a case that for the December 1962 mid-latitude profile the ratio of  $Q/Q_e$  possibly is large enough that the high values of  $T_e$  observed up to 500 km at mid-latitudes could be explained on the basis of the EUV effect and heat conduction in the electron gas. In his interpretation of the daytime altitude behavior of  $T_e$  from the Ariel satellite, Willmore (1963) finds that for altitudes up to 600 km, the altitude dependence of the heat input computed from the observed  $T_e$  and  $N_e$  (cf Equation 1) follows the scale height of atomic oxygen and thus also concludes that the main energy input below 600 km is by the photoionization of atomic oxygen. He additionally finds that the increase of  $T_e$  above 800 km can be explained by additional energy input from the photoelectrons diffusing from below together with the main energy loss mechanism being thermal conduction in the electron gas rather than collisions with positive ions. His conclusions assume that the photoionization of helium is unimportant and additionally depend on an assumed model atmosphere.

#### NIGHTTIME CHARGED PARTICLE TEMPERATURE MEASUREMENTS

The charged particle temperature measurements of Figures 2 and 3 are too sparse and the dependency on the assumed reference atmosphere too critical to draw firm conclusions about departures from temperature equilibrium at night for mid-solar cycle conditions. Bowles et al (1962) observe that  $T_e/T_i$  is unity at night at the geomagnetic equator with  $T_i \cong 600^\circ\text{K}$ , the latter value being in fair agreement with the Harris-Priester reference atmosphere. Remembering the different altitudes and times of the observations, Willmore et al (1963) report that at 1000 km midnight values of  $T_e$  increases from about  $800^\circ\text{K}$  at the equator to  $1400^\circ\text{K}$  at  $60^\circ$  magnetic latitude. Evans (1964) indicates a small but significant

departure from temperature equilibrium in the F region at  $50^\circ$  north magnetic latitude. The definite evidence from the Ariel satellite for quite significant departures from temperature equilibrium at night at medium latitudes have been confirmed by rocket measurements (Brace et al, 1963). The Ariel results show that the nighttime departure from equilibrium becomes more pronounced at the higher latitudes. The nighttime source required to explain the Ariel observations has been estimated to be less than 30 percent of the daytime EUV heat input (Willmore, 1963).

As an example of the sensitivity of nighttime electron temperatures to small sources of heat input, consider Equation (1) and the fact that for solar minimum conditions,  $N_e$  varies by a factor of 4 from day to night at 400 km (Bauer and Blumle, 1964). From these considerations, it can be shown that less than 10 percent of the daytime EUV heat input would be required at night to maintain the same temperature difference ( $T_e - T_i$ ) throughout the day.

#### SUMMARY AND CONCLUSIONS

For all temporal conditions and latitudes, large departures from temperature equilibrium ( $T_e/T_i \geq 2$ ) are observed in the daytime lower F region at the altitude of maximum rate of electron productions. Moderate but significant daytime values for  $T_e/T_i$  are maintained to very high altitudes in winter at mid-latitudes in the middle of the solar cycle. Daytime mid-latitude data taken for summer and/or solar minimum conditions when electron densities generally are much lower reveal much larger values of  $T_e/T_i$  persisting to altitudes well above the F2 maximum. There is considerable evidence at least for altitudes below 600 km that the diurnal electron temperature maximum occurs in the early morning. Observed increases of daytime electron temperature with latitude follows the observed electron density which is under geomagnetic control. All of these temporal and latitudinal trends in the observed electron temperature are consistent with EUV as the predominant daytime source of electron heating. The uncertainties in calculating the EUV effect make it difficult to infer other possible daytime heat sources at the present time. The charged particle temperature observa-

tions strongly suggest the possibility that not all of the EUV energy is locally deposited, an important factor to be considered in the theories of formation of the ionosphere. There is some evidence principally from backscatter experiments that the ion temperature is controlled by electrons at very high altitudes.

Significant departures from temperature equilibrium at night have been observed especially for conditions close to solar minimum. The estimated intensity of this additional heat source increases with latitude but at all latitudes is only a fraction of the daytime EUV effect.

#### ACKNOWLEDGEMENT

The author is grateful to S. J. Bauer, L. J. Blumle, J. V. Evans and K. Bowles, for early access to the results of their charged particle temperature observations.

#### REFERENCES

- AONO, Y., K. HIRAO and S. MIYAZAKI, *Journ. Rad. Res. Labs., Japan*, **9**, 407, 1962.
- AONO, Y., K. HIRAO and S. MIYAZAKI, *Journ. Rad. Res. Labs., Japan*, **8**, 453, 1961.
- BAUER, S. J. and BOURDEAU, R. E., *Journ. Atmos. Sci.*, **19**, 218, 1962.
- BAUER, S. J., *Journ. Geophys. Res.*, **69**, 553, 1964.
- BAUER, S. J., and L. J. BLUMLE, *JGR*, submitted for publication, 1964.
- BOURDEAU, R. E., *Space Research II*, p. 554, 1961.
- BOURDEAU, R. E., *Space Sciences Reviews*, **1**, 683, 1963.
- BOURDEAU, R. E., and DONLEY, J. L., *Proc. Royal Soc. A.*, in press, presented May 1963.
- BOURDEAU, R. E., J. L. DONLEY, E. C. WHIPPLE and S. J. BAUER, *Journ. Geophys. Res.*, **67**, 467, 1962.
- BOWEN, P. J., R. L. F. BOYD, W. J. RAITT and A. P. WILLMORE, *Proc. Royal Soc. A.*, in press, presented May 1963.
- BOWLES, K. L., OCHS, E. R., and GREEN, J. L., *Journ. Natl. Bureau Standards*, **66**, 395 1962.
- BOWLES, K., XIV General Assembly of URSI, Tokyo, September 1963.
- BRACE, L. H., N. W. SPENCER, and G. R. CARIGNAN, *Journ. Geophys. Res.*, **68**, 5397, 1963.
- BRACE, L. H., N. W. SPENCER and A. DALGARNO, AGU, Washington, April 1964.
- DALGARNO A., McELROY, M. B. and MOFFET, R. J., *Plan. & Space Sci.*, **11**, 463, 1963.
- EVANS, J. V. and M. LOEWENTHAL, URSI, Washington, April 1964.
- EVANS, J. V., *Journ. Geophys.* **67**, 4994, 1962.
- GRINGAUZ, K. I., B. N. GEROZHANKIN, N. M. SHUTTI and G. G. GDALEVICI, USSR Geofizicheskaya Sekt., **151**, 560, 1963.
- HALE, L. C., *Journ. Geophys. Res.*, **66**, 1554, 1961.
- HALL, L. A., K. R. DAMON and H. E. HINTEREGGER, *Space Research III*, 1963.
- HANSON, W. B., *Space Research III*, p. 282, 1962.
- HANSON, W. B. and F. S. JOHNSON, *Les Congress et Colloques de L'Université de Liège*, **20**, 390, 1961.
- HANSON, W. B., *Journ. Geophys. Res.*, **67**, 183, 1962b.
- HARRIS, I., and W. PRIESTER, *Space Research III*, p. 58, 1962.
- KING, J. W., P. A. SMITH, D. ECCLES and F. HELM, *Radio Res. Station, I. M.* 94, July 1963.
- LOCKWOOD, G. K. and G. L. NIMS, *Journ. Atmos. Terr. Phys.* 1964, in press.
- SMITH, L. G., *Journ. Geophys. Res.*, **66**, 2562, 1961.
- SPENCER, N. W., BRACE, L. H. and CARIGNAN, G. R., *Journ. Geophys. Res.*, **67**, 157, 1962.
- TAYLOR, H. A., L. H. BRACE, L. C. BRINTON and C. R. SMITH, *Journ. Geophys. Res.*, **68**, 539, 1963.
- WILLMORE, A. P., C. L. HENDERSON, R. L. F. BOYD and P. J. BOWEN, *Proc. Royal Soc. A.*, in press, presented May 1963.
- WILLMORE, A. P., *Proc. Royal Soc. A.*, in press.
- WRIGHT, J. W., *NBS Technical Note*, 138, 1962.